Electronic Thesis and Dissertation Repository

2-22-2024 11:00 AM

Development of an In Vitro Model of Mitochondrial DNA Copy Number Depletion via Stable Inducible Expression of D1135A Mutant DNA Polymerase Gamma

Amanda L. Morin, *Western University*

Supervisor: Castellani, Christina A, *The University of Western Ontario*
A thesis submitted in partial fulfillment of the requirements for the Master of Science degree in Pathology and Laboratory Medicine
© Amanda L. Morin 2024

Follow this and additional works at: https://ir.lib.uwo.ca/etd

Part of the Biology Commons, Genomics Commons, and the Molecular Genetics Commons

Abstract

Mitochondria are responsible for several crucial cellular processes and contain their own DNA (mtDNA) that exists in several copies. Variation of mtDNA copy number (mtDNA-CN) alters energy metabolism and can modify the epigenome and transcriptome. We hypothesized that inducible expression of polymerase-deficient D1135A dominant-negative DNA polymerase gamma (DN-POLG) would result in mtDNA-CN depletion. Here, an *in vitro* model expressing D1135A POLG was created using the Flp-In™ T-REx™-293 stable inducible expression system. Stable integration was confirmed with PCR amplification and Sanger sequencing of post-integration genomic sequences. D1135A POLG expression was confirmed with Western blot of the FLAG-tag antibody. Induction of D1135A POLG expression with tetracycline for 24 hours resulted in reproducible decreases in mtDNA-CN. This model will be used in the future by the Castellani Lab to interrogate the effects of mtDNA-CN depletion on the nuclear epigenome, transcriptome, and metabolome.

Keywords

Mitochondrial DNA copy number, genome editing, stable inducible expression, D1135A POLG polymerase mutant

Summary for Lay Audience

Mitochondria are involved in many cell functions, including energy production. Mitochondria contain their own DNA (mtDNA) that exists in several copies per cell. Variation of mtDNA copy number (mtDNA-CN) alters energy production and has been shown to modify the nuclear epigenome, altering expression of nearby genes. mtDNA is replicated by DNA polymerase gamma (POLG). Different regions (domains) of the POLG protein are responsible for mtDNA editing (exonuclease domain) and replication (polymerase domain). Mutations in the polymerase domain have been shown to decrease mtDNA-CN in cell culture. We hypothesized that expression of polymerase-deficient D1135A POLG would result in mtDNA-CN depletion. A cell model expressing D1135A POLG was created using the Flp-In^{TM} T-REx^{TM}-293 cell line, which contains a Flp-recombinase target (FRT) site and allows the D1135A sequence to be incorporated into the genome via transfection with a plasmid also containing a FRT site. Stable integration of the gene of interest into the Flp-In^{TM} T-REx^{TM}-293 cell line was confirmed with PCR amplification and Sanger sequencing of DNA sequences unique to the cell line after integration. D1135A protein expression was confirmed with Western blot of the FLAG-tag antibody. D1135A POLG expression was induced with tetracycline treatment for 24 hours, resulting in reproducible decreases in mtDNA-CN. This model will be used in the future by the Castellani Lab to interrogate the effects of mtDNA-CN depletion on the nuclear epigenome, transcriptome, and metabolome.

Acknowledgments

Table of Contents

List of Tables

List of Figures

List of Plates

List of Abbreviations

2HG: 2-hydroxyglutarate

Acetyl CoA: acetyl coenzyme A

ACL: ATP citrate lyase

aKG: alpha ketoglutarate

ASPA: aspartoacylase

ATP: adenosine triphosphate

BGH: bovine growth hormone

CVD: cardiovascular disease

DCM: dilated cardiomyopathy

DEG: differentially expressed gene

DMR: differentially methylated region

DNMT: DNA methyltransferase

DN-POLG: dominant-negative DNA polymerase gamma

EWAS: epigenome-wide association study

FAD: flavin adenine dinucleotide

FH: fumarate hydratase

FITR: Flp-In^{TM} T-REx^{TM}-293 cells

FRT: Flp recombinase target

GABA: gamma-aminobutyric acid

GAPDH: glyceraldehyde 3-phosphate dehydrogenase

GO: Gene Ontology

HAT: histone acetyltransferase

HDAC: histone deacetylase

HEK293: human embryonic kidney cells

HMT: histone methyltransferase

IDH: isocitrate dehydrogenase

JMJD: Jumonji-C domain

KO: knockout

mtDNA: mitochondrial DNA

mtDNA-CN: mitochondrial DNA copy number

mtDSB: mitochondrial DNA double strand break

NAA: N-acetylaspartate

NAD: nicotinamide adenine dinucleotide

OXPHOS: oxidative phosphorylation

PAH: polyaromatic hydrocarbon

PCR: polymerase chain reaction

POLG: DNA polymerase gamma

qPCR: quantitative polymerase chain reaction

ROS: reactive oxygen species

SAH: S-adenosylhomocysteine

SAM: S-adenosyl methionine

SDH: succinate dehydrogenase

TCA: tricarboxylic acid

TET: ten eleven translocation

TetO: tetracycline operator

TetR: tetracycline operator repressor

TFAM: mitochondrial transcription factor A

UPR: unfolded protein response

Preface

As an Indigenous researcher, I preface this thesis with a positionality statement. It is important for me to position myself among the many aspects of my identity to accurately convey the story of this academic journey.

I am an Indigenous woman of European descent. My father and his ancestors are among the original inhabitants of Turtle Island (North America) as part of the Ojibwe tribe of Anishinaabe peoples. My dad's family is now primarily located either in Wikwemikong Unceded Reserve on Manitoulin Island or the Greater Sudbury Area. My mother's grandfather was French-Canadian, and her grandmother immigrated to Canada from England after the Second World War. My mom's family is now primarily located in Southwestern Ontario.

In the clan system of the Anishinaabe people, there are clashing theories as to whether we historically adopted our mother's clan or our father's clan. I had first adopted my fathers' clan, the eagle, as he has adopted his father's clan, the eagle. Given the confusion arising from the discourse of recent Indigenous scholars, we have opted to adopt our mother's/grandmother's clan as well, the turtle. Members of the eagle clan were originally charged with outgoing international communications and are said to be the most vocal. Members of the turtle clan were originally charged with teaching and healing. I don't believe it is a coincidence that communication and teaching are two things that I am extremely passionate about in my life now.

I grew up with my mom in a small Mennonite-adjacent town and visited my dad on the Island sporadically. I often describe this situation as "growing up white". Because of this, I grew up only with Western ways of knowing, and excelled in Euro-centric classroom settings. Science and math were my best subjects. That said, I have always had a creative, artistic side to myself, and have spent my life fostering a great respect for my relationship with nature. Even with these connections to art and nature in my "white" life, I always felt as if there was a part of my being that was missing.

I was finally connected to my culture through the Indigenous Student Center (formerly Indigenous Services) at Western. Throughout my teachings I learned how to bead, I learned

Creation stories, I learned my language, and I learned the truth about the residential school system. At that point I was extremely interested in genetics, while simultaneously learning about intergenerational trauma in Indigenous communities. Intergenerational trauma is a very real experience for me and my siblings. As children and grandchildren of residential school survivors, we all suffer some sort of mental ailment. I do not believe this is a coincidence.

With recent evidence supporting the heritability of epigenomic signatures, and the knowledge that epigenomic signatures can be altered in response to stress, I came to the realization that epigenomics and genomics is the subject area in which I would like to conduct research. I believe that this research will reveal biological mechanisms of intergenerational trauma, and that the knowledge of these mechanisms will help improve health care for those suffering from intergenerational trauma. This includes North American Indigenous peoples, but also encompasses several other communities that are known to suffer from the consequences of intergenerational trauma, such as members of racially and socially marginalized groups, veterans, domestic abuse survivors, and individuals of the foster care system, to name a few.

Dr. Castellani's work was of great interest to me, as it proposes a mechanism through which stress can alter the epigenome via transgenerational inheritance – through mitochondrial DNA variability. Although I am aware of the complexities of human genetics, and that there is rarely a single contributing factor to certain phenotypical outcomes, the connection between matrilinear inheritance of mitochondrial DNA and the real existence and experiences with intergenerational trauma sparked a flame in me. While there are several factors that affect the state of the nuclear epigenome, there is an abundance of significant results linking mitochondrial DNA variation to the nuclear epigenome, with subsequent gene expression alterations that have implications in health and disease. Further, during my studies in the Castellani lab, other research groups have specifically studied the role of intergenerational trauma in mitochondrial DNA variation and resultant epigenomic changes. I was enamored by the fact that I could contribute to such a significant and relatively young area of genetic research while also feeling like my research could contribute to Indigenous communities in a meaningful way.

Throughout my academic journey, I struggled with the reconciliation of the many parts of my identity. Many of my Indigenous peers talk very negatively about Europeans and are

disenchanted with the scientific method and academia. Out of the ~150 Indigenous graduate students at Western, I am one of the very few students who is enrolled in a STEM program. I spent a significant amount of time concerned that my passion for science would create a certain reputation for myself within the Indigenous community. I was worried that I would not be welcome.

This academic journey was not a means to an end for me. It was an incredible chapter of my life story that I will look back on fondly. I will be forever grateful to Christina Castellani for taking me on as her first Masters student.

Chapter 1

1   Introduction

The mitochondrion is a double membrane-bound organelle involved in several essential cellular processes, including fatty acid synthesis (1), calcium regulation (2), reactive oxygen species (ROS) signaling (3), and apoptosis (4), among others. Perhaps the most crucial function of the mitochondrion is energy production in the form of adenosine triphosphate (ATP) via the interconnected tricarboxylic acid (TCA) cycle and oxidative phosphorylation (OXPHOS), as shown in Figure 1. This process provides the cell with most of its energy and can produce up to 90% of the cells' ATP in highly metabolic tissues, such as cardiac muscle cells (5).

In addition to its role in energy production, the TCA cycle is also involved in several metabolic pathways and signaling cascades via its metabolic intermediates, such as citrate, succinate, fumarate, nicotinamide adenine dinucleotide (NAD+), flavin adenine dinucleotide (FAD), acetyl co-enzyme A (acetyl CoA) and alpha ketoglutarate (αKG). OXPHOS, particularly complex I and II activity, regulates the TCA cycle as these complexes oxidize NADH and $FADH_2$ to NAD+ and FAD, respectively. NAD+ and FAD act as electron acceptors and are essential for the proper function of the TCA cycle. As such, the mitochondria are heavily implicated in the metabolism of the cell and have been referred to as the "metabolic hub of the cell" (6). As the metabolic hub of the cell, mitochondria are involved in several cellular processes beyond mitochondrial processes and are also implicated in pathogenesis of diseases, such as neurodegenerative diseases (6), cancer (7), and cardiovascular diseases (8).
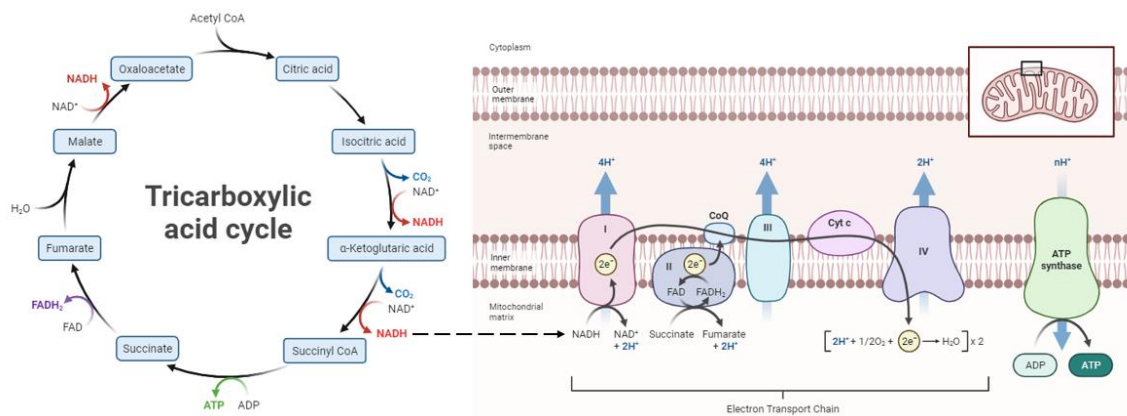
Figure 1. The tricarboxylic acid (TCA) cycle (left) and oxidative phosphorylation (OXPHOS, right). Nicotinamide adenine dinucleotide (NADH) generated in the TCA cycle is directly fed into OXPHOS at complex I where it is oxidized to NAD+ to be used again in the TCA cycle. Adapted from "Electron Transport Chain" and "Kreb's Cycle", by BioRender.com (2023). Retrieved from https://app.biorender.com/biorender-templates.

Mitochondria contain their own genome (mtDNA) that is haploid, maternally inherited, non-intronic and 16,569 base pairs long. The genome codes for 13 proteins contributing to four of the five OXPHOS enzymatic complexes, as well as 22 tRNA molecules and two rRNA molecules required for mitochondrial protein translation. Mitochondrial gene expression varies across different cells and tissues (9). Nuclear genes code for >99% of the mitochondrial proteome; as such, crosstalk between the nuclear and mitochondrial genomes is essential for cell function (10).

Compared to the nuclear genome which exists in two copies per cell, mtDNA exists in several copies per cell, a metric of mtDNA quantity referred to as mtDNA copy number (mtDNA-CN). A single cell can contain up to thousands of mitochondria, with each mitochondrion containing 2-10 copies of mtDNA (11). Basal mtDNA-CN is determined by cell and tissue type; cells and tissues with increased metabolic demands have a higher basal mtDNA-CN compared to cells and tissues of lower metabolic demands. For example, human skeletal muscle has a higher basal mtDNA-CN compared to human lung epithelial tissue (12). Levels of mtDNA-CN are higher in females, are associated with frailty and all-cause mortality (13), and are associated with self-rated health status (14).

Another metric of mtDNA quality is called heteroplasmy, which is defined as the ratio of mutant to wildtype mtDNA present in a cell. Heteroplasmic burden refers to the ratio of mutated to non-mutated mtDNA molecules present in a cell. There are two scenarios of heteroplasmic burden: 1) heteroplasmic burden of a single mtDNA mutation; and 2) global heteroplasmic burden, indicating mutations across the entire mitochondrial genome. Global heteroplasmic burden increases with age and is reported to be lower in females (15,16). Due to the lack of introns and protective histones, as well as the proximity to ROS generated by OXPHOS, mtDNA is more susceptible than nuclear DNA to damage. Skeletal cells from related and unrelated healthy individuals at different ages all possessed variants in both the D-loop (i.e. control) region and coding regions of mtDNA at >0.2% heteroplasmy, suggesting the human mtDNA universally exists in a heteroplasmic state (17). Single mtDNA mutations can result in mitochondrial disease (18). With pathogenic mtDNA mutations, the cell can tolerate a high frequency of the pathogenic variant before mitochondrial disease manifests, known as the biochemical

threshold (19). Maintaining mitochondrial genomic integrity (mtDNA-CN and heteroplasmy) is essential for cell function.

A landmark study published by Smiraglia and colleagues in 2008 showed that complete mtDNA-CN depletion resulted in significant genome-wide hyper- and hypomethylation that was almost completely restored upon the reintroduction of wild type mtDNA (20). In the years since, several other groups have revealed the association between mtDNA-CN variation in DNA methylation as well as other epigenomic processes, such as histone methylation (21) and acetylation (22). A proposed mechanism of this association is that mtDNA-CN variation results in mitochondrial dysfunction, altering cellular metabolism and modulating epigenome-modifying metabolites (23). Furthermore, these epigenomic changes seen in response to mtDNA-CN variation have been shown to be associated with transcriptomic changes (24) in genomic regions associated with complex disease (25,26).

1.1   Mito-nuclear crosstalk is essential for cell function

Because >99% of the mitochondrial proteome is encoded by nuclear DNA, and because mitochondria are heavily implicated in cellular metabolic processes, communication between the nucleus, the mitochondria and their genomes is essential for proper cell function (10). Furthermore, communication between these organelles and their genomes is essential to offset cellular dysfunction and return to homeostatic conditions (27). This mito-nuclear crosstalk can be referred to as anterograde signaling, where the nucleus sends signals to the mitochondria, or as retrograde signaling, where mitochondria send signals to the nucleus. Mito-nuclear crosstalk is also essential for more specialized cell functions as well, such as specialization and differentiation (28).

Nuclear encoded genes code for all but 13 mitochondrial proteins (29). Maintaining the integrity of the nuclear genome and epigenome is therefore essential to maintain mitochondrial function. In turn, the maintenance of mitochondrial function is essential both for the overall function of the cell, as well as the maintenance of the nuclear epigenome. Mitochondrial activity during the S-phase of the cell cycle targets mitochondrial enzymes to the nucleus to alter epigenetic marks that make cell cycle-related genes accessible during DNA replication (30). In embryogenesis, maternal

cytoplasmic factors regulate development (31) until metabolites, enzymes and transport signals generated by mitochondrial function initiate zygotic gene activation (32).

There is some evidence of pathways available to repair mtDNA double-stranded breaks (mtDSBs) (33) however most evidence suggests that there are no repair pathways for mtDSBs (34). As such, when a mtDSB occurs, certain signals are sent to the nucleus to ensure there are no disruptions to cellular function; one study showed an upregulation of cell-cycle checkpoint protein p21 (35), while another study showed an upregulation of interferon-stimulated genes, indicating that mtDSBs may illicit an immune response (36). Furthermore, mild mitochondrial stress induces the mitochondrial unfolded protein response (UPR) which alters import efficiency, allowing for transcription factors to migrate to the nucleus and induce expression of stress-related genes (37).

1.2   Mitochondrial DNA copy number and mitochondrial function

Variation in mtDNA-CN perturbs mtDNA gene expression and affects mitochondrial function. Generally, decreasing mtDNA-CN negatively affects mitochondrial function; conversely, increasing mtDNA-CN enhances mitochondrial function (38). Increased mtDNA-CN is associated with an increase in mitochondrial gene expression and typically correlates with an increase in mitochondrial function (39). This rise in mtDNA-CN is regularly seen in embryogenesis and differentiation (24). Natural variation in mtDNA-CN is seen across tissues and between individuals and can influence mitochondrial function. For example, human skeletal muscle samples with a higher mtDNA-CN display increased activity of mtDNA-encoded OXPHOS complex proteins (40). Although increased mtDNA-CN enhances mitochondrial function, this may not always be a positive scenario for the cell. If there is substantial mtDNA damage, the cell will upregulate mtDNA-CN to compensate for perturbed mitochondrial function, as is the case for several human cancers (41). A unique scenario in which increased mtDNA-CN is detrimental to the cell is in the male gamete, where sperm concentration, motility, and overall quality decreases if mtDNA-CN exceeds ~100 copies (42).

Decreased mtDNA-CN is associated with decreased expression of mtDNA-encoded OXPHOS complex subunits, inhibition of complex I, III, IV and V activity, and limited

ATP production (20). Disruption of gene expression and inhibition of OXPHOS complex activity compromises cellular respiratory capacity (43). Cells with low mtDNA-CN show partial OXPHOS defects and prioritize glutamine metabolism for chemical energy production, indicating a marked change in mitochondrial and cellular metabolism (44). Furthermore, inhibiting complex I activity increases superoxide production, which can damage mtDNA and lead to further dysfunction (45). OXPHOS replenishes NAD+ pools for the TCA cycle; inhibition of OXPHOS complex activity via mtDNA-CN decrease perturbs TCA cycle activity, altering the metabolic state of the cell (22).

Because mitochondrial metabolites can act as substrates and co-factors for epigenomic processes (23), mtDNA-CN variation can also alter the state of the nuclear epigenome.

1.3   The nuclear epigenome

The nuclear epigenome describes chemical modifications to nuclear DNA and its histones that contribute to regulation of gene expression independent of the DNA sequence. Common chemical modifications to nuclear DNA and histones include methylation and acetylation. Methylation involves the transfer of a methyl group (—CH3). In DNA methylation, a methyl group is transferred to the C5 carbon of a cytosine residue followed by a guanine residue (CpG site, p=phosphate backbone). This transfer is mediated by a group of enzymes called DNA methyltransferases (DNMTs) (46). Conversely, DNA demethylation removes the methyl group from the CpG site and is mediated by the Ten Eleven Translocation (TET) family of enzymes. DNA methylation in promoter regions has been shown to repress gene expression (47). In histone methylation, a methyl group is transferred to an amino acid residue of any of the four histone proteins (H2A, H2B, H3, H4), a process mediated by histone methyltransferases (HMTs). Histone demethylation removes the methyl group from the amino acid residues and is mediated in part by Jumonji-C domain (JMJD) family of enzymes. Histone methylation can promote or repress gene expression depending on the amino acid residue that is methylated, and the number of methyl groups present (48). Histones, but not DNA, are also modified by acetylation, which involves the transfer of an acetyl group (—COCH3) to a lysine residue of any of the four histone proteins. This transfer is mediated by histone acetyltransferases (HATs). Histone deacetylation removes the acetyl group

from the lysine residue and is mediated by a group of enzymes called histone deacetylases (HDACs). Histone acetylation is associated with promotion of gene expression, due to acetyl groups neutralizing the positive charge of the histone, causing the histone to drift away from the DNA (48).

The epigenome alters gene expression without changing the genetic code. Thus, the epigenome contributes to an organism's phenotype. As such, epigenome-wide association studies (EWAS) can be performed to derive and identify associations between quantifiable epigenetic marks and identifiable phenotypes, such as disease (49).

1.3.1 Mitochondrial DNA copy number and the nuclear epigenome

Mitochondrial DNA copy number variation is associated with epigenomic changes, primarily DNA methylation and histone methylation and acetylation (50). An abundance of evidence linking mtDNA-CN variation and nuclear DNA methylation comes from *in vitro* models of mtDNA-CN variation. One such model targets mitochondrial transcription factor A, a mtDNA binding protein essential in mtDNA replication encoded by the nuclear *TFAM* gene. Dr. Castellani developed three independent *TFAM* knockout (KO) HEK293 cell lines in the Arking Lab at Johns Hopkins University that exhibited an 18-fold reduction in mtDNA-CN (25). Epigenomic analysis of *TFAM* KO cells revealed 4,242 differentially methylated sites, 228 differentially methylated regions, and 179 differentially expressed genes compared to controls (results generated by Castellani lab members Phyo Win and Julia Nguyen, manuscript under review). Additionally, Dr. Castellani previously performed an EWAS using methylation data from three cardiovascular disease (CVD) cohorts and identified CpGs significantly associated with mtDNA-CN; these CpGs were further validated in the *TFAM* knockout cell line (25). Our group performed an additional EWAS and meta-analysis of mtDNA-CN association with DNA methylation which revealed CpGs to be significantly associated with mtDNA-CN across multiple ethnicities in five cohorts (26). Further, results from Gene Ontology (GO) analysis of the EWAS samples and *TFAM* KO cell lines suggest that mtDNA-CN drives changes in nuclear DNA methylation at sites near genes relating to cell-signaling processes (25).

The association between mtDNA-CN and the nuclear epigenome has also been examined in tissues extracted from human subjects. For example, in sperm cells, mtDNA-CN was associated with 218 differentially methylated regions (51). Differential methylation is seen in glioblastoma tumor cells containing ~0-3% mtDNA-CN compared to glioblastoma cells containing 100% mtDNA (44). Mitochondrial DNA copy number variation can lead to mitochondrial dysfunction via inhibited mitochondrial protein translation (43), triggering mitochondrial superoxide production. Superoxide mediates the modification of several histone acetylation marks, including H3K9 and H3K14 (52). mtDNA-CN reduction leads to decreased histone deacetylase (HDAC) activity, which increases histone H3K27 acetylation in gene promoters, likely triggering chromatin activation (53). mtDNA reduction also invokes a decrease in acetylation marks for H2B, H3 and H4 histones, though acetylation of these histones can be rescued upon TCA cycle restoration (22).

1.4 Mitochondrial DNA copy number and epigenome-modifying metabolites

Mitochondrial DNA variation is associated with changes in cellular metabolism, likely via modulating epigenome-modifying metabolites and the state of the nuclear epigenome, including DNA and histone methylation/acetylation changes (50).

The mechanisms of the relationship between mtDNA-CN variation, mitochondrial function and the nuclear epigenome are yet to be elucidated. It has been proposed that this relationship exists through mitochondrial metabolites that are known to be substrates and co-factors for epigenome-modifying processes. While several metabolites can alter the nuclear epigenome, methionine, S-adenosylmethionine (SAM), S-adenosylhomocysteine (SAH), NAD+, acetyl CoA, and αKG are crucial to mitochondrial metabolism and are well-studied in their roles contributing to DNA and histone methylation and histone acetylation. The enzymatic interactions and resultant epigenome modifications are outlined in Table 1.

Table 1. Summary of selected metabolites, enzymatic interactions, and related epigenomic modification upon increase of the metabolite.

Metabolite	Enzymatic Interaction	Epigenomic modification
Methionine	Substrate for MAT, required for SAM production	Promotes DNA methylation
SAM	Substrate for DNMTs; activates activity	Promotes DNA methylation
SAH	Substrate for DNMTs; inhibits activity	Inhibits DNA methylation
α-ketoglutarate	Co-factor for TET and JMJD demethylases	Promotes DNA (TET) and histone (JMJD) demethylation
Acetyl CoA	Substrate for HATs	Promotes histone acetylation
NAD+	Co-factor for sirtuins	Promotes histone deacetylation

*MAT: methionine adenosyltransferase; SAM: S-adenosyl methionine; DNMT: DNA methyltransferase; SAH: S-adenosyl homocysteine; TET: ten-eleven translocation; JMJD: jumonji C domain; HAT: histone acetyltransferase; NAD: nicotinamide adenine dinucleotide

Studies of a well-known pharmaceutical, metformin, provide evidence that epigenomic changes could be mediated by mitochondrial function. Metformin is used to treat type II diabetes mellitus, a metabolic disorder characterized by insulin insufficiency and perturbed glucose metabolism, and therefore perturbed mitochondrial function. Epigenome analysis of type II diabetes patients taking metformin compared to those not taking metformin revealed a number of differentially methylated regions (54). Metformin significantly decreases SAH levels, thus increasing SAM levels, promoting DNA methylation (54). Metformin does not modify DNA methylation in cells depleted of their mitochondria, suggesting that metformin contributes to epigenomic changes via mitochondria and mtDNA-CN (55).

The one-carbon cycle, also referred to as the folate cycle, includes reactions which occur both in the cytoplasm but also primarily in the mitochondria. This cycle reflects the transfer of one carbon from either serine or glycine generating methionine and/or key contributors to RNA and DNA (56). Via methionine, the one-carbon cycle contributes to the production of SAM. Thus, the one-carbon cycle can indirectly affect methylation through alteration of SAM, a methyl donor used in DNA methylation. These dynamics are evidenced by mtDNA-CN depletion triggering expression of key synthesis genes and enzymes of the one-carbon cycle and encouraging homocysteine remethylation (57,58). Furthermore, mtDNA-CN depleted cells alter metabolism to produce serine from glucose (59). When glucose is metabolized to serine, intermediates of the TCA cycle and OXPHOS are modulated to compensate, for example decreasing pools of αKG, contributing to hypermethylation via decreased TET demethylase activity (60). The serine metabolism pathway fuels the methionine salvage pathway to help regenerate cellular levels of SAM (61), whose increase also contributes to hypermethylation (62). Glucose metabolism can be altered by administration of 2-deoxyglucose; upon administration, global histone acetylation is altered, pointing towards glucose availability and mitochondrial function contributing to epigenomic changes (63).

The majority (70%) of acetyl CoA is derived from mitochondrially metabolized glucose; mtDNA-CN depletion results in diminished acetyl CoA pools, reduced HAT activity, and loss of histone acetylation peaks (64). The rest of cellular acetyl CoA is derived from

other chemical sources, such as N-acetylaspartate (NAA) and citrate. NAA is an amino acid derivative formed by the anabolism of aspartic acid and acetyl CoA. NAA is metabolized to aspartic acid and acetyl CoA via aspartoacylase (ASPA) activity and is a reaction that can replete both acetyl CoA and aspartic acid pools. When ASPA expression is knocked down, the abundance of acetyl CoA pools decreases (65), which likely stalls the TCA cycle, resulting in decreased histone acetylation. Citrate is an intermediate of the TCA cycle that is generated by acetyl CoA and oxaloacetate metabolism. It is metabolized to acetyl CoA by ATP-citrate lyase (ACL); deletion of *ACLY,* the nuclear gene encoding ACL, results in a switch from glucose to acetate metabolism and genome-wide histone deacetylation (66).

Because mtDNA-CN can modulate metabolites of the TCA cycle (i.e. NAD+ via complex I proteins encoded by mtDNA), mtDNA-CN variation also exerts its effect on TCA cycle enzymes. *IDH* codes for isocitrate dehydrogenase, an NAD+-dependent enzyme responsible for converting isocitrate into αKG and a key enzyme of the TCA cycle. Altering or inhibiting IDH activity contributes to mitochondrial dysfunction, as is the case in many cancers where *IDH* mutations are present (67,68). Altered IDH activity further metabolizes αKG to 2-hydroxyglutarate (2HG), which competes with αKG to inhibit the function of αKG-dependent enzymes, including TET demethylases, resulting in a significant increase in DNA methylation (68). 2HG dehydrogenases are evolutionarily conserved enzymes that metabolize 2HG back into αKG, mitigating the effects of mutant *IDH* and contributes to the reversal of hypermethylation (69). Mitochondrial superoxide, a primary by-product of oxidative stress, further contributes to mitochondrial dysfunction via inhibition of IDH activity resulting in accumulation of citrate and acetyl CoA and depleted αKG pools (70). This accumulation of acetyl CoA contributes to histone acetylation and transcriptional activation (71). Furthermore, this inhibition of isocitrate metabolism to αKG increases NAD+ pools since reduction of NAD+ to NADH happens concurrently to the oxidation of isocitrate. Other TCA cycle enzymes also contribute to the dynamics of the nuclear epigenome through modulation of metabolites. Succinate dehydrogenase (SDH) metabolizes succinate into fumarate, and fumarate hydratase (FH) metabolizes fumarate into malate. Succinate and fumarate are competitive inhibitors for both αKG and 2HG and will preferentially bind to histone

demethylases and TET DNA hydroxylases, increasing genome-wide histone and DNA methylation (21). Variation of cellular metabolism through the TCA cycle and OXPHOS plays an essential role in the dynamics of the nuclear epigenome.

1.5 Mitochondrial DNA copy number in health and disease

Mitochondrial DNA variation and mitochondrial function greatly contribute to disease outcomes. Mitochondrial dysfunction is implicated in several human diseases, including cancer (72), diabetes (73), cardiovascular disease (CVD) (74), HIV/AIDS (75), multiple sclerosis (76), Alzheimer's, Parkinson's, Huntington's (6), autism (77), and schizophrenia (78). Mitochondria are also implicated as drivers of aging phenotypes (35,79). There is a clear association that exists between mitochondrial function and disease, and mitochondrial function and aging. Due to the role mtDNA-CN variation plays in mitochondrial function and dysfunction, mtDNA-CN can be used as a biomarker of mitochondrial function in health and disease (40).

Mitochondria are heavily implicated in the pathogenesis of cancer (80). A hallmark of cancer cells is the Warburg effect, wherein the cell metabolizes glucose primarily through glycolysis in the presence of oxygen (81). Often, nuclear-encoded mitochondrial genes are mutated in cancer, for example, isocitrate dehydrogenase (*IDH*), a key enzyme in the TCA cycle (52,67,68). Conversely, tumours require extensive energy, as such requires a sufficient level of mtDNA-CN for tumorigenesis to occur (67). Glioma patients whose tumors contained a higher mtDNA-CN had better prognoses than patients whose tumor had a lower mtDNA-CN (11).

Obesity is a complex disease that arises from excessive accumulation of adipose tissue either through poor lifestyle and diet or metabolic syndrome. Obese patients have been shown to have a lower mtDNA-CN than their average-weight counterparts, which was also associated with the differential methylation of metabolic genes (82). Lower mtDNA-CN is also associated with insulin resistance, a risk factor for the development of diabetes mellitus type 2 (83).

Cells of cardiac tissue have high basal mtDNA-CN, likely due to high energy demands; studies of mitochondrial contribution to cardiac-related diseases are plentiful. Studies across multiple cohorts and ethnicities show that low mtDNA-CN in peripheral blood samples is associated with increased risk for hypertension (84), incident heart failure (85), and incident atrial fibrillation (86). In a study of dilated cardiomyopathy (DCM) patients, lactate production was 5.4-fold higher in DCM patients than controls, and elevated αKG levels were seen (87). This may reflect a switch in metabolism towards the TCA cycle to compensate for decreased energy metabolism through anaerobic glycolysis. In a mouse model of heart failure, mtDNA-CN decreased by ~40% in failing myocardium after myocardial infarction (88). In another mouse model, symptoms of cardiomyopathy due to dominant-negative DNA polymerase gamma (DN-*POLG)* transgene expression were confirmed (89), and in another model, DN-*POLG* transgene expression led to left ventricle hypertrophy that progressed into cardiogenic heart failure (90).

Mitochondria play a significant role in the pathogenesis of neurodegenerative diseases (Alzheimer's, Huntington's, Parkinson's). Sufficient energy is required for the survival of neurons; mtDNA-CN decreases with age, reducing energy production and potentially contributing to neurodegenerative diseases (6). Indeed, a meta-analysis of 9 cohorts of individuals with Alzheimer's disease and healthy controls showed that the circulating blood of individuals with Alzheimer's disease had significantly lower mtDNA-CN compared to healthy controls, and that circulating mtDNA-CN could be used as a biomarker for Alzheimer's disease (91). In another study comparing mtDNA-CN of individuals with Huntington's disease and healthy controls, leukocytes and fibroblasts from individuals with Huntington's diseases showed a decrease in mtDNA-CN compared to healthy controls (92). Similarly, mtDNA-CN was lower in peripheral blood, substantia nigra tissue and frontal cortex tissue in individuals with Parkinson's disease compared to healthy controls and was deemed a biomarker of Parkinson's disease (93).

Recently, mitochondria have been implicated in other neurological disorders. Peripheral blood samples from patients with bipolar disorder revealed a higher mtDNA-CN compared to controls, and the increased mtDNA-CN was associated with advanced

epigenetic age (94). Post-mortem hippocampal samples of patients with bipolar disorder also had increased mtDNA-CN associated with advanced epigenetic age (95). Similarly, peripheral blood samples from patients with major depressive disorder revealed a higher mtDNA-CN compared to controls (96). Schizophrenia is a complex neurological disorder that is discordant among monozygotic twins ~50% of the time. Analysis of whole blood samples from patients with schizophrenia revealed both an increase and decrease in mtDNA-CN compared to the healthy twin and compared to healthy controls (97), highlighting the complex interactions that occur between mtDNA-CN, mitochondrial function, and disease pathogenesis.

1.6 Mitochondrial DNA and the environment

Mitochondria are known to relay important information about the health of the cell to the nucleus, where the appropriate response can be initiated. Due to mitochondria's sensitivity to changes in cellular metabolism, the genomes sensitivity to DNA damage, and the ability for exogenous factors to alter metabolism, it is important to consider the relationship between exogenous factors, mtDNA variation and their combined effects on the restructuring of the nuclear epigenome.

Mitochondrial DNA copy number varies in response to a variety of environmental factors. Some lifestyle factors such as obesity have been shown to decrease mtDNA-CN (82), while alcohol consumption and cigarette smoking can lead to mtDNA deletions (98,99). E-cigarette smoking has been shown to increase mtDNA-CN (100). Many environmental pollutants such as heavy metals and polyaromatic hydrocarbons can increase mtDNA-CN (101,102). Life-saving pharmaceuticals such as the HIV antiretroviral drug Zidovudine significantly decrease mtDNA-CN (103), and stressful life events have been suggested to modify mtDNA (104).

Exogenous factors may be able to exert their effects on mtDNA and the nuclear epigenome across generations. Stress, especially long-term stress, is known to induce the release of cortisol from the adrenal glands, resulting in changes in glucose metabolism and mitochondrial function (105). Mice pups born to mothers who were stressed by exposure to a predator scent four days before birth showed significant increases in 2HG,

succinate, and gamma-aminobutyric acid (GABA) in brain tissue; these are all important metabolites for the mitochondrial TCA cycle (106). A study out of Mexico City observed the effects of a natural disaster on cord blood mtDNA-CN in three cohorts of children born to women who: a) conceived and gave birth to a child before a devastating earthquake, b) conceived before the earthquake and gave birth after the earthquake, and c) conceived and gave birth after the earthquake. Infants from each of the three groups had a significant difference in umbilical cord blood mtDNA-CN, with the first group having the lowest copy number and the third group having the highest number (104). A study out of China showed that prenatal exposure to polycyclic aromatic hydrocarbons (PAHs) resulted in an elevated mtDNA-CN in umbilical cord blood (102). Similarly, prenatal exposure to manganese (101) and aluminum (107) resulted in an elevated mtDNA-CN in cord blood. Evidence presented shows that altered metabolism and mtDNA-CN are seen across generations in response to stress, and therefore could suggest a potential mechanism for the transmittance of intergenerational trauma.

1.7   DNA polymerase gamma (POLG)

Because the mitochondrial genome does not code for any DNA polymerases, mitochondrial genomic integrity is maintained by nuclear encoded genes. DNA polymerase gamma (POLG), consisting of one catalytic and two accessory subunits, is solely responsible for mtDNA replication and repair. The catalytic subunit of DNA polymerase gamma is encoded by the *POLG* gene located on the q arm of chromosome 15. The POLG protein has a total of 1239 amino acids with a molecular weight of 140kDa that comprises an accessory interacting domain, an intrinsic processivity domain, and two functional domains (Figure 2). The two functional domains are the 3'-5' exonuclease domain and the polymerase domain, responsible for base-pair editing and DNA replication, respectively. The POLG protein is the only molecule responsible for mtDNA replication and is also the only molecule contributing to proofreading during replication, unlike in the nucleus where several DNA polymerases and repair proteins are in action (108). As such, mutations in the polymerase domain of POLG negatively affects mtDNA-CN as there is no other polymerase to compensate. Several experiments have

identified that a D1135A alteration in the polymerase domain of POLG reduces mtDNA-CN (109–111).

Figure 2. Functions and structure of the catalytic subunit of DNA polymerase gamma, encoded by nuclear *POLG* (112). The N-terminal domain (denoted TD) contains the mitochondrial targeting sequence. Thumb (Th) subdomains are present between the exonuclease and linker regions as well as the polymerase region. The linker region contains the accessory interacting domain (AID) and the intrinsic processivity (IP) domain. The exonuclease domain contains essential motifs I, II and III. The polymerase domain contains subdomains comprising the Thumb (Th), Palm and Finger, which contains motifs A, B and C.

It has been reported that D1135A POLG exhibits a dominant negative phenotype, where the activity of the mutant protein product interferes with the activity of the wild-type protein product. Inducible expression of polymerase-deficient D1135A POLG resulted in a 50% decrease in mtDNA-CN with each cell division (111). As such, the D1135A POLG alteration is referred to as DN-POLG.

1.8 Flp-In^{TM} T-REx^{TM} System for stable inducible expression

The Flp-In^{TM} T-REx^{TM} System allows for the generation of stable mammalian cell lines exhibiting tetracycline-inducible expression of a gene of interest from a specific genomic location. This system utilizes Flp-In^{TM} T-REx^{TM}-293 cells, which are modified human embryonic kidney (HEK293) cells containing a Flp Recombinase Target (FRT) site, constitutive Tetracycline Operator Repressor (TetR) expression, and zeocin and blasticidin resistance genes for selection. Flp-In^{TM} T-REx^{TM}-293 cells are available for purchase from ThermoFisher.

The Flp-In T-REx^{TM}-293 cell line is co-transfected with the pOG44 and the pcDNA^{TM}5/FRT/TO plasmids. The pOG44 plasmid contains an ampicillin resistance gene for plasmid propagation and selection in *E. coli* as well as the gene expressing Flp-recombinase (Figure 3A). The pcDNA^{TM}5/FRT/TO plasmid contains an FRT site, two tetracycline operators, a multiple cloning site for insertion of a gene of interest, and an ampicillin resistance gene for selection (Figure 3B).

The expression of Flp recombinase from the pOG44 vector mediates the recombination between the FRT site present in the Flp-In^{TM} T-REx^{TM}-293 genome and the FRT site present on the pcDNA^{TM}5/FRT/TO vector. Upon successful recombination, the gene of interest under tetracycline operator control as well as the hygromycin resistance gene are stably integrated into the genome. This recombination event shifts the zeocin resistance gene out of the correct reading frame. Therefore, successful integration of the expression vector results in cells exhibiting blasticidin and hygromycin but not zeocin resistance, a phenotype unique to the host Flp-In^{TM} T-REx^{TM}-293 cells that can be used for selection purposes.
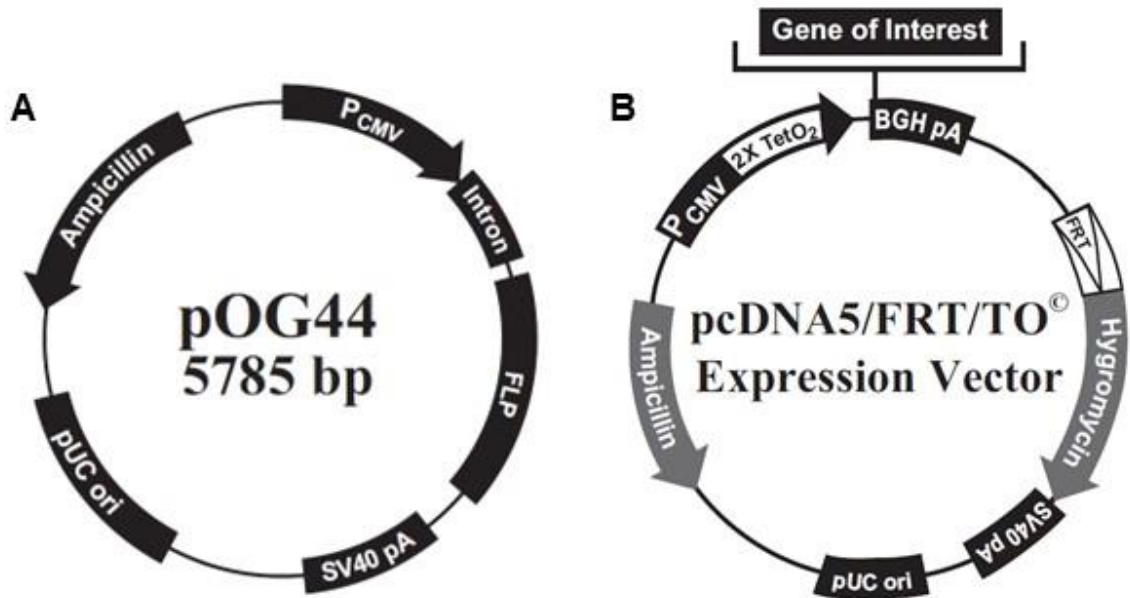
Figure 3. Plasmid maps **A:** the pOG44 expression vector expressing Flp recombinase, and **B:** the pcDNA^TM^5/FRT/TO expression vector (113). The Flp recombinase target (FRT) site is flanked by the BGH polyadenylation signal and hygromycin resistance gene. Gene of interest is dominant-negative POLG (DN-POLG).

The series of genomic features is unique to the cell line after successful integration of the gene of interest. Before integration, the FRT site in the Flp-In^{TM} T-REx^{TM}-293 genome has a SV40 promoter upstream and the zeocin resistance gene downstream (Figure 4). Similarly, the FRT site present on the expression vector is preceded by the bovine growth hormone (BGH) polyadenylation signal upstream and the hygromycin resistance gene downstream (Figure 3B). After successful integration, two FRT sites are present in the genome, and are surrounded by a different set of genomic features. The FRT site present in the genome is flanked by the BGH polyadenylation signal upstream and the zeocin resistance gene downstream. Similarly, the FRT site from the expression plasmid that is integrated into and present in the host cell genome, is flanked by the SV40 promoter upstream, and the hygromycin resistance gene downstream (Figure 5). These features flanking the two FRT sites now present in the genome can be utilized to create primers to amplify these unique post-integration sequences to confirm successful integration of the expression plasmid into the genome. Upon successful integration of the pcDNA^{TM}5/FRT/TO expression vector into the host cell genome, cells can be treated with tetracycline to induce expression of the gene of interest (Figure 6).
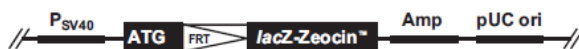
Figure 4. Genomic features flanking the Flp recombinase target (FRT) site present in the Flp-In^{TM} T-REx^{TM}-293 genome before integration of the gene variant of interest (113).

Figure 5. Series of genomic features present in the post-integration genome of Flp-In^{TM} T-REx^{TM}-293 cells (113). The Flp recombinase target (FRT) site on the left is flanked by the SV40 promoter and hygromycin resistance gene; the FRT site on the right is flanked by the BGH polyadenylation signal and *lac*Z-Zeocin resistance gene.
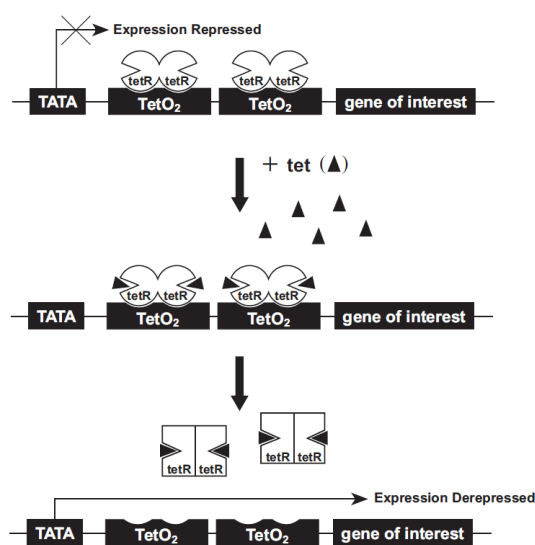
Figure 6. Overview of a tetracycline-inducible expression system (113). In the absence of tetracycline, tetracycline operator repressors (TetR) bind to the tetracycline operator (TetO), repressing expression of the gene of interest. In the presence of tetracycline, TetR binds to tetracycline, changes conformation and releases from TetO, allowing expression of the gene of interest.

1.9   Hypothesis and Aims

There is an abundance of evidence suggesting mtDNA integrity plays a critical role in the maintenance of the nuclear epigenome. mtDNA-CN variation has been shown to be associated with changes in DNA methylation and histone acetylation patterns, subsequently altering gene expression. The mechanisms of these associations have yet to be elucidated.

It is hypothesized that inducible expression of polymerase-deficient D1135A dominant-negative DNA polymerase gamma (DN-POLG) will result in mtDNA-CN depletion. This hypothesis is tested with the following aims: (1) to confirm mutations in expression vectors and create a stable, inducible expression system to alter levels of mtDNA-CN in culture; (2) to confirm successful integration of the plasmid containing the gene of interest into the genome; and (3) to treat D1135A POLG cells with tetracycline and measure resultant mtDNA-CN.

Chapter 2

2 Methods and Materials

2.1 Cell Culture

HEK293 cells (ATCC CRL-1573^{TM}) were cultured in high glucose Dulbecco's Modified Eagle Medium (DMEM, Gibco #11965118) supplemented with 10% fetal bovine serum (FBS, Gibco #12483020) and 1% penicillin-streptomycin (PenStrep, Gibco #15140122) at 37˚C and 5% CO_2. Flp-In^{TM} T-REx^{TM}293 cells (ThermoFisher #R78007) were cultured in complete HEK293 media (DMEM + 10% FBS + 1% PenStrep) supplemented with 100µg/mL zeocin (Gibco #R25005) and 15µg/mL blasticidin (Gibco #A1113903) at 37˚C and 5% CO_2. DN-POLG cells were cultured in complete HEK293 media supplemented with 100µg/mL hygromycin (Gibco #10687010) and 15µg/mL blasticidin at 37˚C and 5% CO_2. All experiments were run in technical triplicates unless otherwise stated.

2.2 pcDNA^{TM}5/FRT/TO expression vectors

Expression vectors (pcDNA^{TM}5/FRT/TO) containing the genes of interest (WT *POLG*, D198A *POLG*, D1135A *POLG*) were generated by GeneArt (Thermo Scientific). Each gene of interest is amended at the N-terminus with 2x FLAG tags to allow for detection of the integrated POLG protein. The WT-POLG vector contains a wild-type POLG sequence and is not expected to alter heteroplasmy or mtDNA-CN upon induction of expression. The D198A vector contains the *POLG* gene mutated in the DNA region coding for the exonuclease domain, inducing heteroplasmy upon induction of expression of the POLG protein. The D1135A POLG vector contains the *POLG* gene mutated in the DNA region coding for the polymerase domain, reducing mtDNA-CN upon expression of the POLG protein.

2.3 Bacterial transformation and plasmid purification

Plasmid DNA was transformed into One Shot® MAX Efficiency® DH5α^{TM}-T1^{R} Competent *E. coli* cells (ThermoFisher #12297-016). For each plasmid (pOG44, pcDNA^{TM}5/FRT/TO ×3), 1µg of DNA was added directly to vials of *E. coli* cells and

incubated on ice for 30 minutes. Vials were incubated at 42˚C for 30s then transferred back on ice. Warmed SOC (**S**uper **O**ptimal broth with **C**atabolic repression) media was added to each vial and incubated with shaking at 37˚C for 1 hour. Cells were diluted 1:10 and plated on 100mm LB agar plates containing 100µg/mL ampicillin. Plates were inverted and incubated at room temperature for five days. Colonies were inoculated into LB broth containing 100µg/mL ampicillin and cultured at 37˚C with shaking for 16 hours. Plasmid purification was achieved using QIAprep Spin Miniprep Kit according to manufacturer's protocol (Qiagen #27104). Purified plasmid DNA quality and concentration was determined using Nanodrop 2000 (Thermo Scientific).

2.4 Generation and maintenance of stable inducible DN-POLG cell lines

One day prior to transfection, Flp-In™ T-REx293™ cells were plated in a 6-well plate at a density of 800 000 cells per well in complete media containing 15µg/mL blasticidin. Cells were co-transfected using Lipofectamine3000 (Invitrogen) according to manufacturer's protocol with a 9:1 ratio of pOG44 vector (2.25µg) and pcDNA5/FRT/TO expression vector (0.25µg). Twenty-four hours later, cells were washed with Dulbecco's Phosphate Buffered Saline (DPBS, Gibco #14190144) and media was replaced with fresh complete media containing 15µg/mL blasticidin. Forty-eight hours after transfection, one half of cells were split to 25% confluency in media containing 15µg/mL blasticidin and 100µg/mL hygromycin (Plate 1). One half of cells were split to 25% confluency in complete media containing 15µg/mL blasticidin; after twenty-four hours, media was replaced with complete media containing 15µg/mL blasticidin and 100µg/mL hygromycin (Plate 2). Every three days, cells were washed, and selection media was replaced to maintain cell lines. Twenty-one days after transfection, cells were split to 25% confluency in T75 flasks and passaged every 4-5 days. All cell lines were created according to this method.
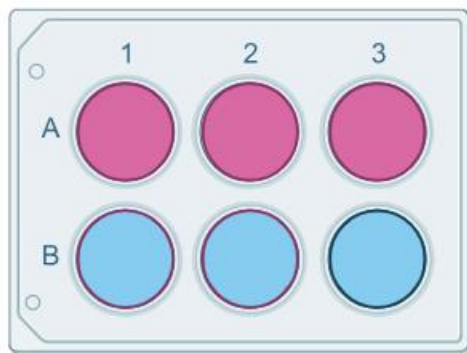
Plate 1. Forty-eight hours after transfection, cells were split to 25% confluency in media containing 15µg/mL blasticidin and 100µg/mL hygromycin. A1: WT-POLG; A2: D198A POLG; A3: D1135A POLG; B1: Flp recombinase control; B2: Negative control; B3: No treatment control.
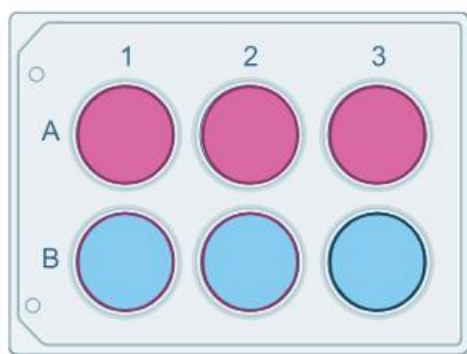
Plate 2. Forty-eight hours after transfection, cells were split to 25% confluency in media containing 15µg/mL of blasticidin for 24 hours, after which media was replaced with media containing 15µg/mL blasticidin and 100µg/mL hygromycin. A1: WT-POLG; A2: D198A POLG; A3: D1135A POLG; B1: Flp recombinase control; B2: Negative control; B3: No treatment control.

While three cell lines were created, only the D1135A POLG cell line was used for experiments. Due to time constraints and the scope of this project, D198A POLG cells will be characterized by a future Castellani lab trainee.

2.5 Tetracycline treatments

Flp-In^{TM} T-REx^{TM} and D1135A POLG cells were plated into 6-well plates at 700 000 cells per well in complete DMEM supplemented with 100µg/mL hygromycin and 15µg/mL blasticidin. Forty-eight hours after plating, media was replaced with complete DMEM containing hygromycin and blasticidin supplemented with tetracycline (Gibco #A39246). Twenty-four hours after tetracycline treatment, cells were harvested for DNA and protein extraction.

2.6 Phenol-chloroform-isoamyl alcohol DNA extraction and ethanol precipitation

Cells were washed with DPBS and treated with Trypsin-EDTA 0.05% (Gibco #25300062) to detach cells. Cells were resuspended in complete DMEM and centrifuged at 500 X g for 5 minutes to pellet cells. Cells were lysed using RLT Buffer Plus (Qiagen #1053393). An equal volume of UltraPure^{TM} phenol:chloroform:isoamyl alcohol (25:24:1, Invitrogen #15593031) was added to the lysed cells. Samples were thoroughly vortexed and subsequently centrifuged for 15 minutes at 17 000*xg* and the aqueous phase was collected into a new microfuge tube. ***Ethanol precipitation:*** Glycogen (20µg/µL, Invitrogen #10814010), sodium acetate (3M pH 5.2, Thermo Scientific #R1181) and ice-cold 100% ethanol were added to the aqueous sample at the following volumes and in the following order:

1. Glycogen: 1µL

2. Sodium acetate: 0.1X original sample volume (µL)

3. 100% ethanol: 2.5X (sample volume + sodium acetate volume) (µL)

After an overnight period at -20˚C, samples were centrifuged for 20 minutes at 17 000 X g and 4˚C to pellet DNA. Supernatant was discarded, DNA pellet was washed with ice-

cold 70% ethanol and samples centrifuged at 17 000 X g and 4˚C. This step was performed twice before resuspending the DNA pellet in UltraPure™ Water (Invitrogen #10977015). DNA quality and quantity was determined on the Nanodrop 2000 (Thermo Scientific). If 260/230 values were outside the range of 1.8-2.2, ethanol precipitation (without glycogen) was repeated.

2.7   PCR primer design

PCR primers were designed using Primer Blast (NCBI). Forward and reverse primers for WT, D198A, and D1135A POLG expression plasmids were generated by inputting either a random wild-type sequence (WT POLG) or the mutated *POLG* sequence (D189A and D1135A *POLG*) as the input PCR template. The D198A and D1135A primer sets were targeted to amplify the pcDNA™5/FRT/TO expression plasmid ~150bp upstream and downstream of the *POLG* mutation. The WT POLG primer sets were targeted to create an <400bp PCR amplicon in any region along the DNA sequence. Breakpoint primers (FRT-Hygro, FRT-Zeo) were designed to amplify the FRT sites present in the genome after successful integration (Figure 7). Characteristics of all primer sets are described in Table 2.

Figure 7. Placement of breakpoint primer sets, FRT-Hygro (FWD and REV) and FRT-Zeo (FWD and REV). The sequence of the Flp-In™ T-REx™ -293 nuclear genome after integration of the pcDNA™5/FRT/TO vector was generated in UGENE (Unipro) using pFRT/lacZ-Zeo expression plasmid and pcDNA™5/FRT/TO expression plasmid sequences. The assembled sequences were then input into Primer Blast, and forward and reverse primers were created to amplify the FRT site. Primer sets with the most similar melting temperatures were selected for use. FRT-Hygro-FWD primer was designed to anneal to the SV40 promoter while the REV primer was designed to anneal to the hygromycin resistance gene to amplify the flanked FRT site. Similarly, FRT-Zeo-FWD primer was designed to anneal to the BGH polyadenylation signal, while the REV primer was designed to anneal to the *lacZ*-Zeocin resistance gene, amplifying the flanked FRT site.

Table 2. Characteristics of primers designed for amplification of integrated genes of interest and integration breakpoints.

Primer Name	Sequence	Amplicon length
WT-FWD	5'-TGAGGGCACATGTCCTACACT-3'	271bp
WT-REV	5'-GCATAGACATGGTGTCCAGGAA-3'	
D198A-FWD	5'-GGCCCAACTGCCTCCAAAAC-3'	278bp
D198A-REV	5'-CTGTAGGCACTTCCAGAGGAATC-3'	
D1135A-FWD	5'-GCAGAGCCCTTGAACCTAGC-3'	389bp
D1135A-REV	5'-TCTTCTTTCCATGCCGGTGG-3'	
FRT-Hygro-FWD	5'-GATTGGGAAGACAATAGCAGGC-3'	454bp
FRT-Hygro-REV	5'-AAGGGCGATCGGTGCG-3'	
FRT-Zeo-FWD	5'-CCTAACTCCGCCCAGTTCC-3'	516bp
FRT-Zeo-REV	5'-TAGGTCAGGCTCTCGCTGAA-3'	

2.8   PCR and agarose gel electrophoresis

PCR amplification of DN-POLG mutations and FRT breakpoints was performed in a 50µL reaction volume containing 50ng of DNA, PCR buffer, 1.5mM MgCl$_2$, 200µM of dNTPs, 0.5µM each of forward and reverse primer, and 2.5 units Taq polymerase. PCR reactions were denatured at 95˚C for 1 minute, followed by 35 cycles of denaturation at 95˚C for 15s, annealing at 55˚C for 15s, and extension at 72˚C for 15s. A final extension step was performed at 72˚C for 7 minutes and reactions were held at 4˚C. PCR amplified DNA amplicons were resolved on a 1% agarose gel in 1X tris-boric acid-EDTA (TBE) buffer at 100V for 1.5 hours. The gel was incubated in TBE buffer containing 0.5µg/mL ethidium bromide for 30 minutes with periodic agitation and imaged using UV light on the ChemiDoc XRS+ (Bio-Rad). PCR reactions were cleaned using the QIAquick Gel Extraction Kit (Qiagen #28704) according to manufacturer's protocol and prepared for Sanger sequencing.

2.9   Sanger Sequencing

To prepare for Sanger sequencing, DNA quality and quantity of PCR reactions were determined using a Nanodrop 2000 (Thermo Scientific). PCR reactions were diluted to 5ng/uL. WT, D198A and D1135A FWD and REV primers were diluted to 2.0µM. Each Sanger sequence reaction contained 10µL of PCR amplified DNA and 5µL of each primer. Sanger sequencing was performed at the London Regional Genomics Center at Robarts Research Institute (Western University).

2.10 qPCR for mtDNA-CN estimation

mtDNA-CN is estimated with quantitative polymerase chain reaction (qPCR) by using primer sets targeting both the nuclear and mitochondrial genomes. This assay utilizes Albumin primers (nuclear target) and D-Loop primers (mitochondrial target) and quantitation qPCR settings to determine the cycle threshold (Ct) of each primer set, which are described in Table 3. Nuclear genes exist in only two copies while mitochondrial genes exist in several copies, therefore a known stable nuclear gene (albumin) is used as a one copy reference gene to establish the relative amount of mtDNA. The Ct value of the mitochondrial target will be expected to be lower than that

of the nuclear target. Delta Ct values between albumin and D-Loop therefore give a proxy measurement of mtDNA-CN relative to the nuclear copy number of the nuclear target. Here, mtDNA-CN was determined using real-time qPCR assay using SYBR chemistry in a 10μL reaction. This protocol was adapted from Hsieh *et. al* (114) and optimized in the Arking Lab at Johns Hopkins University and the Castellani Lab at Western University.

Each reaction contained 5μL of 2X PowerTrack SYBR Green Master Mix (Thermo Scientific #A46109), 2μL (10ng/μL) of genomic DNA, 1uM each of forward and reverse primer, and filled to 10μL water. Genomic DNA was quantified using Qubit (Invitrogen). For experiments ran in technical triplicate, the thermocycling program began with a 95°C enzyme activation for 15 minutes, followed by 45 cycles of denaturation at 94°C for 15s, annealing at 62°C for 10s, and elongation at 74°C for 19s. Data was collected at 62°C. For experiments ran in biological and technical triplicate, the thermocycling program began with a 95°C enzyme activation for 15 minutes, followed by 45 cycles of denaturation at 94°C for 15s, D-loop primer annealing at 62°C for 10s, D-loop extension at 74°C for 19s (D-loop signal acquisition occurs here), albumin annealing at 84°C for 10 seconds, and albumin extension at 88°C for 19s (albumin signal acquisition occurs here).

Table 3. Nuclear albumin and mitochondrial D-Loop qPCR primer sequences.

Primer	Forward sequence	Reverse sequence
Albumin	5' - **CGG CGG CGG GCG GCG CGG GCT GGG CGG*** AAA TGC TGC ACA GAA TCC TTG - 3'	5' - **GCC CGG CCC GCC GCG CCC GTC CCG CCG*** GAA AAG CAT GGT CGC CTG TT – 3'
D-Loop	5' - *ACG CTC GAC ACA** CAG CAC TTA AAC ACA TCT CTG C – 3'	5' - *GCT CAG GTC ATA** CAG TAT GGG AGT GRG AGG GRA AAA – 3'

*Bold text represents GC clamps; italic text represents non-complementary bases; R denotes degenerate A/G bases (50%/50%).

2.11 Total protein extraction and Western blot

For all cell lines, cells were pelleted at 500xg for 5 minutes, washed with 5mL of DPBS and pelleted again. Total protein lysates were extracted using ice-cold radioimmunoprecipitation assay (RIPA) lysis buffer supplemented with EZBlock™ Protease and Phosphatase Inhibitor (BioVision #AB201120). Protein concentration was

quantified using the Pierce[TM] BCA Protein Assay Kit (Thermo Scientific #23225) and lysates were stored at -80˚C. Proteins were diluted to equal concentration, mixed with an equal volume of 2X Laemmli sample buffer (Bio-Rad #1610737) supplemented with 5% mercaptoethanol and resolved on an 8% polyacrylamide gel at 120V for 1.5 hours. The first lane was loaded with Multi-Color Pre-Stained Protein Standard (GenScript #M00624-250). Proteins were transferred to a 0.45µm nitrocellulose membrane using the Trans-Blot® Cell system at 80V for 2 hours. The membrane was cut such that the target protein was contained to one piece of membrane and the control protein was contained to the other piece of membrane. Membranes were blocked in 5% skim milk in tris buffered saline with 0.1% Tween20 (TBS-T) overnight at 4˚C, rinsed with TBS-T and then incubated with primary antibody at room temperature for one hour. After washing membranes five times with TBS-T, membranes were incubated in secondary antibody at room temperature for one hour. Antibodies used are described in table 4. Membranes were washed five times with TBS-T before incubation in SuperSignal[TM] West Pico PLUS Chemiluminescent Substrate (Thermo Scientific #34577). Membranes were realigned and imaged on the ChemiDoc XRS+ (Bio-Rad) using the "Chemi" setting for protein bands and "Colorimetric" setting for protein ladder. Images were exported and merged using Adobe Photoshop "Overlay" feature. Densitometry analysis was performed using ImageJ. Bands were isolated and chemiluminescent intensity of the target band was normalized against control.

Table 4. Primary and secondary antibodies used for Western blotting.

Primary antibody target (dilution)	Host Species	Company (catalog #)	Secondary antibody (dilution)
FLAG-tag (1:5000)	Rabbit	GeneScript (A00170)	Goat anti-rabbit (1:50 000)
GAPDH (1:5000)		Invitrogen (PA5-75762)	

2.12 Statistical analysis

Linear regression analysis for qPCR estimation of mtDNA-CN compared to control sample D1135A POLG NC was performed in RStudio version 2023.09.1 (R version 4.3.2). To determine significant mtDNA-CN changes across concentrations, linear

regression analysis was performed compared to each concentration. Differences are statistically significant at values of $p < 0.05$.

Statistical analysis of Western blot was performed using one-sample T-test in GraphPad PRISM version 10.1.0. Data is presented as means +/- SEM. Statistical significance is set at $p < 0.05$.

Chapter 3

3   Results

To create a stable inducible expression system using the Flp-In^{TM} T-Rex^{TM}-293 system, the pcDNA^{TM}5/FRT/TO expression vector containing the gene of interest was generated for co-transfection with the pOG44 expression vector. Empty pcDNA^{TM}5/FRT/TO expression vectors are available for purchase, allowing users to conduct their own protocols to insert a mutated gene into the multiple cloning site of the expression vector. We confirmed successful integration as well as measured resulting mtDNA-CN levels and protein expression which we describe in this chapter.

3.1   pcDNA5^{TM}/FRT/TO expression vectors harbour expected DN-POLG mutations

Three pcDNA^{TM}5/FRT/TO plasmids were designed and purchased through GeneArt (Thermo Fisher): 1) Wild-type POLG (WT-POLG); 2) Exonuclease-deficient POLG (D198A POLG); and 3) Polymerase-deficient POLG (D1135A POLG). The plasmids were generated based on the native human POLG amino acid sequence and a DNA sequence was generated that had the same GC content and codon usage as humans but was distinguishable from the human wild-type *POLG* gene sequence. The 5' DNA appendix for the *POLG* sequence was *BamHI* restriction site and a Kozak sequence, and the 3' DNA appendix was a stop codon and *NotI* restriction site; this allows for cloning of the *POLG* sequence into the pcDNA^{TM}5/FRT/TO vectors. Plasmids were optimized to avoid the following cis-acting sequence motifs: 1) internal TATA boxes, chi-sites and ribosomal entry sites; 2) AT- or GC-rich sequence stretches; 3) RNA instability motifs; 4) repeat sequences and secondary structures; and 5) splice donor and acceptor sites.

Given that POLG plasmid residues harboured unique DNA sequences, PCR primers that were expected to amplify the integrated *POLG,* but not native wild-type *POLG* were generated. To confirm the presence of the DNA mutations giving rise to D198A and D1135A POLG protein in the appropriate pcDNA^{TM}5/FRT/TO expression plasmid and the absence of mutations in the WT-POLG expression plasmid, plasmid DNA was subject to PCR amplification using primers as described in Table 1 (WT-POLG, D198A

POLG, D1135A POLG). Each plasmid was subject to PCR amplification using one of three primer sets to confirm that the relevant mutation was present only in the appropriate plasmid and confirm POLG sequence integrity. PCR amplicons were visualized on a 1% agarose gel incubated in ethidium bromide (Figure 8). WT, D198A and D1135A primers produced amplicons 271bp, 278bp, and 389bp in length, respectively. PCR reactions were cleaned via a kit method, quantified, diluted, and sent with primers for Sanger sequencing to The London Regional Genomics Center (LRGC). Sanger traces confirmed that the WT-POLG plasmid does not contain D198A or D1135A *POLG* mutations (Figures 9A and 9B, top), while the D198A and D1135A POLG plasmid contained their respective *POLG* mutations, both resulting in an amino acid modification from aspartic acid to alanine at amino acid position 198 (Figure 9A, bottom) and 1135 (Figure 9B, bottom), respectively.
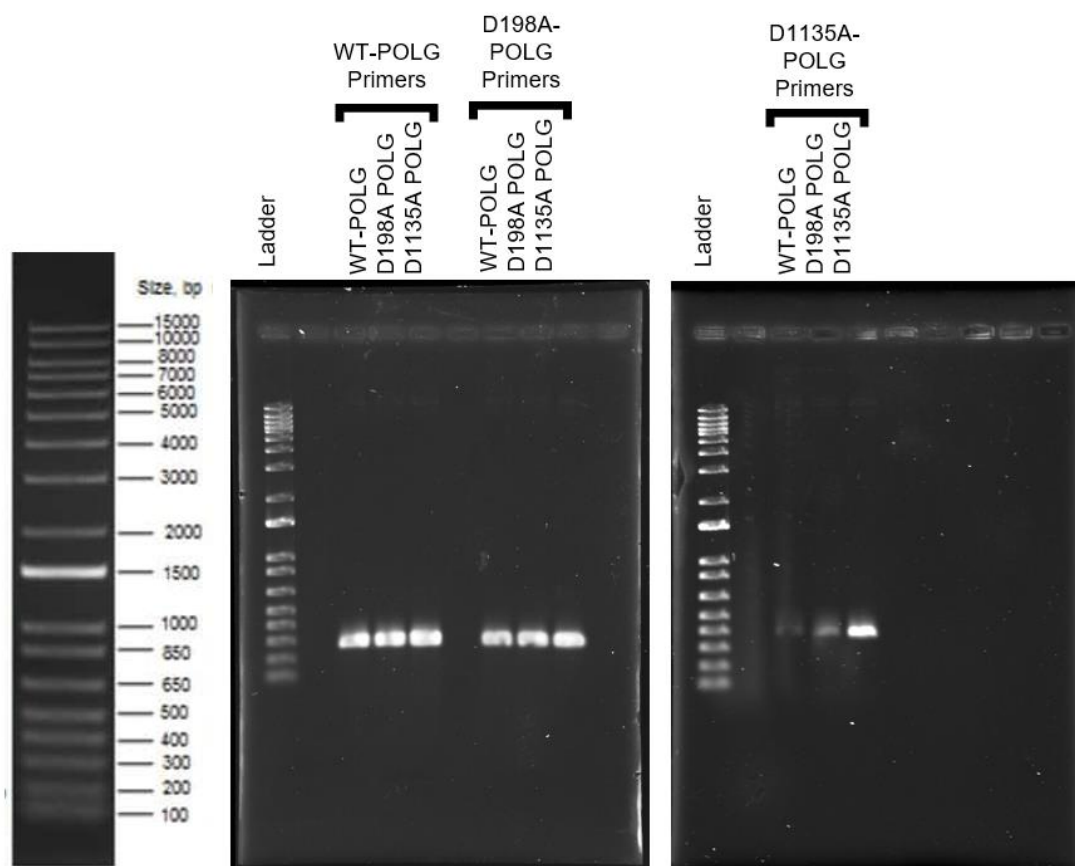
Figure 8. PCR amplicons visualized on 1% agarose gel. WT-POLG primers produced an amplicon 271bp in length, D198A POLG primers produced an amplicon 278bp in length,

and D1135A POLG primers produced an amplicon 389bp in length, as described in Table 2.
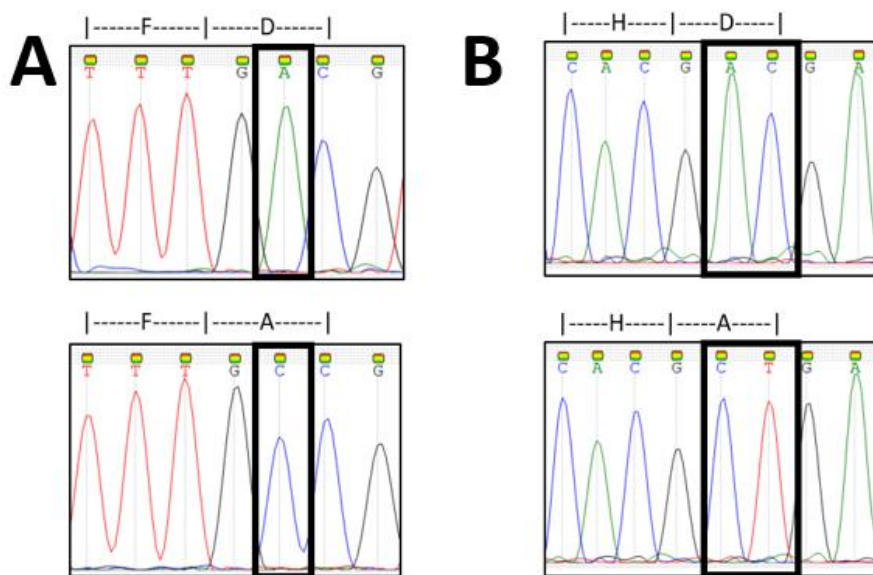
Figure 9. Sanger traces confirming the presence of *POLG* mutations in the plasmid DNA, giving rise to DN-POLG protein products. **A:** The WT sequence (top) translates to aspartic acid (D) at amino acid 198 while the DN-POLG D198A sequence (bottom) translates to alanine (A) at amino acid 198. **B:** The WT sequence (top) translates to aspartic acid (D) at amino acid 1135 while the DN-POLG D1135A sequence (bottom) translates to alanine (A).

3.2 pcDNA5^{TM}/FRT/TO vectors successfully integrated into the genome of Flp-In^{TM} T-REx^{TM}-293 cells

Prior to Flp-mediated integration of the gene of interest into the Flp-In^{TM} T-REx^{TM}-293 cell genome, the FRT site present in the genome is preceded by the SV40 promoter upstream and followed by the *lac*Z-Zeocin resistance gene downstream (figure 4), while the FRT site present on the expression plasmid is preceded by a BGH polyadenylation signal upstream and followed by the hygromycin resistance gene downstream (figure 3B). After successful integration of the gene of interest in the Flp-In^{TM} T-REx^{TM}-293 genome, the FRT site originally present in the cell genome is now preceded by the BGH polyadenylation signal and followed by the *lac*Z-Zeocin resistance gene, while the FRT site present on the plasmid is now incorporated into the genome and is preceded by the SV40 promoter and followed by the hygromycin resistance gene. Primers were designed to amplify these unique post-integration genomic features around the integrated FRT sites and not the FRT site present in non-integrated cells, or the FRT site present in any remaining plasmid DNA. Genomic DNA was extracted from DN-POLG cells growing in complete DMEM containing 100µg/mL hygromycin and 15µg/mL blasticidin. DNA (50ng) was PCR amplified using primers as described in Table 2 (FRT-Zeo, FRT-Hygro). PCR amplicons were resolved and visualized on a 1% agarose gel (Figure 10). Amplification of WT, D198A and D1135A *POLG* genomic DNA with FRT-Zeo primers produced amplicons 454bp in length as described in Table 2. Amplification of WT, D198A and D1135A *POLG* genomic DNA with FRT-Hygro primers produced amplicons 516bp in length. The original PCR reactions were cleaned, and quantity determined to ensure there was sufficient DNA available for sequencing.
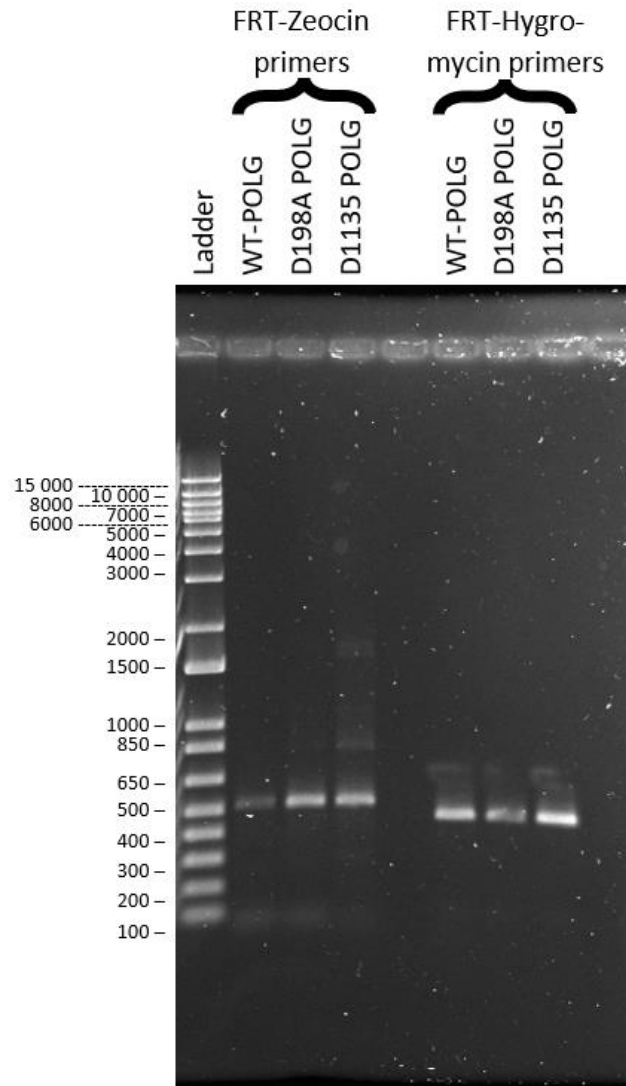
Figure 10. PCR amplicons from DN-POLG cell lines using FRT breakpoint primers as described in Table 2. FRT-Zeo primers produced a 516bp amplicon in WT, D198A and D1135A POLG cell lines; FRT-Hygro primers produced a 454bp amplicon in WT, D198A and D1135A POLG cell lines.

Sanger traces were aligned with sequences of the targeted unique genomic features and annotated, which confirmed the presence of these unique genomic features only in integrated cells. The FRT-Zeo primers successfully amplified the FRT site present in the genome post-integration (Figure 11), while the FRT-Hygro primers successfully amplified the FRT site from the expression plasmid now present in the genome post-integration (Figure 12), confirming successful independent integration of the expression plasmids into the Flp-In^{TM} T-REx^{TM}-293 genome.
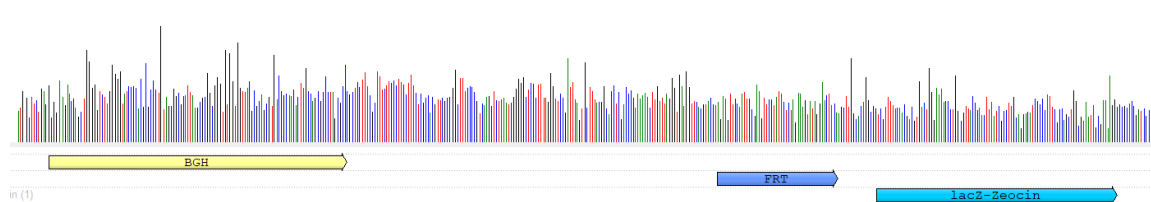
Figure 11. Annotated Sanger trace of the breakpoint sequence wherein the BGH polyadenylation signal is upstream of the FRT site and the *lacZ*-Zeocin gene is downstream of the FRT site.
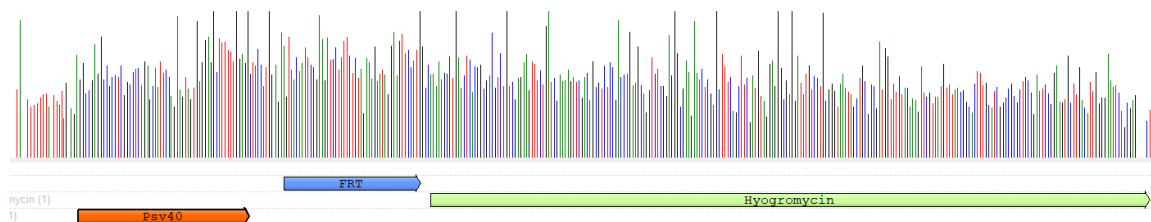
Figure 12. Annotated Sanger trace of the breakpoint sequence wherein the SV40 promoter is upstream of the FRT site, and the hygromycin resistance gene is downstream of the FRT site.

While the generation of the D198A POLG and D1135A POLG cell lines were confirmed via sequencing of the breakpoint primers, only the D1135A cell line was used for further experiments, as described in section 2.4. After confirming integration of the gene of interest into the genome and several passages, the D198A cell line did not reach confluency at the same rate as the D1135A cell line. Additionally, D198A cell viability was decreasing with each passage. The culture conditions were identical between the cell lines. It was evident that viability was decreasing with every passage, as was the growth rate compared to D1135A POLG cells. Lack of sufficient growth of the D198A cell line will be addressed in the future thus this line was omitted from further experiments in this thesis.

3.3 Tetracycline-induced expression of D1135A POLG depletes mtDNA-CN

The Flp-In^{TM} T-REx^{TM} protocol suggests treating cells with 1.0µg/mL of tetracycline to induce expression of the gene of interest. However, the protocol also suggests treating cells with a range of tetracycline concentrations to optimize and modulate expression of the gene of interest (113). I hypothesized that treating cells with increasing concentrations of tetracycline would increase D1135A POLG expression, resulting in concentration-dependent mtDNA-CN depletion. To that end, D1135A POLG cells were treated with 0.5, 1.0, 1.5, 2.0 and 2.5 µg/mL of tetracycline for 24 hours. Flp-In^{TM} T-REx^{TM}-293 cells as well as D1135A POLG cells with no tetracycline exposure were used as controls. Genomic DNA was extracted for mtDNA-CN estimation via qPCR analysis (Figure 13). Linear regression analysis and fold-change calculated with ΔΔCt values reveals the following: mtDNA-CN was depleted by 63% when cells were treated with 0.5µg/mL of tetracycline (p=1.46e-06), 70% when treated with 1.0µg/mL (p=8.80e-07), 67% when treated with 1.5µg/mL (p=4.34e-07), 68% when treated with 2.0µg/mL (p=2.40e-07), and 55% when treated with 2.5µg/mL (p=1.44e-05). Overall, a 65% reduction in mtDNA-CN was seen following induction (p=5.90e-07), but the reduction was not concentration-dependent. mtDNA-CN of cells treated with 1.0µg/mL, 1.5µg/mL, 2.0µg/mL and 2.5µg/mL tetracycline did not significantly differ from that of cells treated with 0.5µg/mL tetracycline (p=0.228, p=0.361, p=0.174, p=0.133, respectively).

Interestingly, D1135A POLG cells treated with 2.5µg/mL of tetracycline had a significantly higher mtDNA-CN than that of cells treated with 1.0µg/mL, 1.5µg/mL or 2.0µg/mL of tetracycline (p=0.018, p=0.024, p=0.009, respectively).
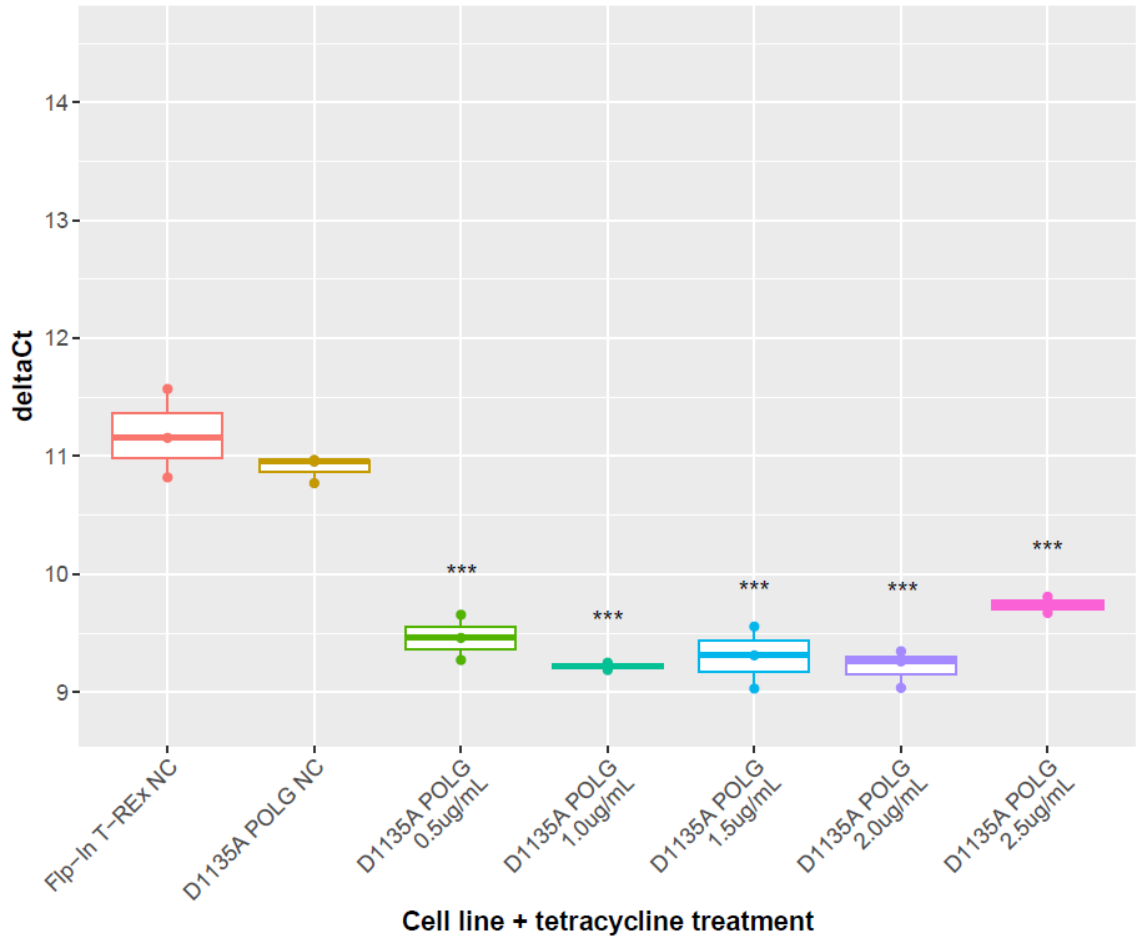
Figure 13. qPCR estimation of mtDNA-CN in D1135A POLG cells treated with 0.5, 1.0, 1.5, 2.0 and 2.5 µg/mL of tetracycline for 24 hours. All doses significantly depleted mtDNA-CN (65% overall reduction, p=5.90e-07). Samples were run in technical triplicates. Asterisks indicate significance compared to D1135A POLG NC: * $p<0.05$, ** $p<0.01$, *** $p<0.001$, linear regression.

3.4 Tetracycline alone leads to low-levels of mtDNA-CN variation in unedited Flp-In™ T-REx™-293 cells

The increase in mtDNA-CN seen at 2.5µg/mL tetracycline was an interesting result. I hypothesized that tetracycline was having an independent effect on mtDNA-CN. Flp-In™ T-REx™ -293 cells were treated with 0.5, 1.0, 1.5, 2.0 and 2.5µg/mL tetracycline for 24 hours, and genomic DNA was extracted for mtDNA-CN estimation via qPCR (Figure 14). An overall small increase in mtDNA-CN is seen across all doses (p=3.135e-06, <1CT). Each tetracycline dose resulted in a significant increase in mtDNA-CN compared to the null control (0.5µg/mL, p=0.034; 1.0µg/mL, p=0.001; 1.5µg/mL, p=5.76e-06; 2.0µg/mL, p=3.66e-07; 2.5µg/mL, p=7.89e-06).
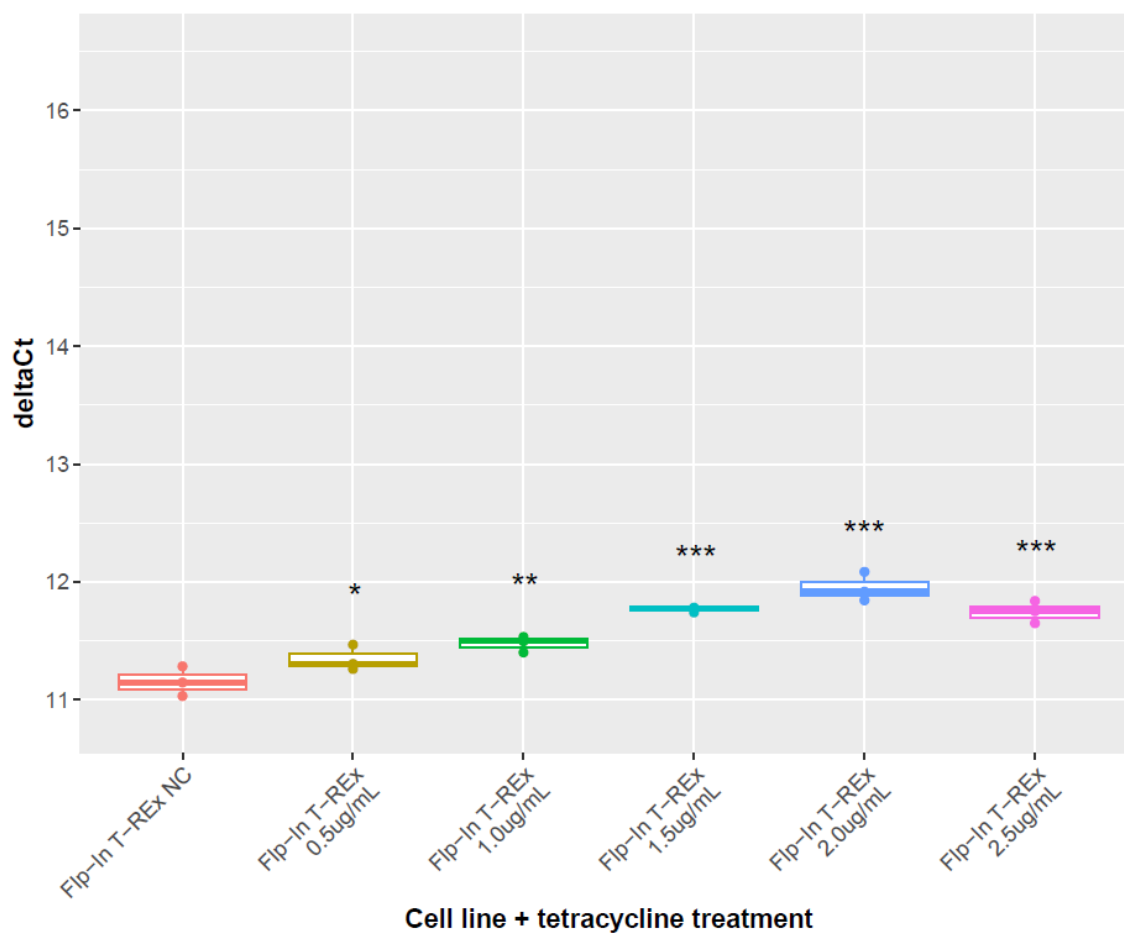
Figure 14. qPCR estimation of mtDNA-CN in Flp-In^TM T-REx^TM-293 cells treated with 0.5, 1.0, 1.5, 2.0 and 2.5 µg/mL of tetracycline for 24 hours. All doses resulted in a significant increase in mtDNA-CN (p=3.13e-06). Samples were run in technical triplicates. Asterisks indicate significance compared to Flp-In T-REx NC: * p<0.05, ** p<0.01, *** p<0.001, linear regression.

Though there is a significant mtDNA-CN increase when Flp-In™ T-REx™-293 cells were treated with 0.5-2.5 µg/mL tetracycline, the effect of D1135A POLG expression on mtDNA-CN represents a much larger decrease of mtDNA-CN at all concentrations (Figure 13). Further, such high doses of tetracycline are not required to induce D1135A POLG expression, since treating cells with 0.5µg/mL of tetracycline is sufficient to reduce mtDNA-CN by 63%. As such, the positive effects of tetracycline on mtDNA-CN can be considered negligible. However, to account for these effects, final results were normalized for the effect of tetracycline. Treating Flp-In™ T-REx™-293 cells with 0.5µg/mL of tetracycline resulted in a 5% increase in mtDNA-CN (p=0.034). Because the effect of tetracycline was not determined at every concentration used, the 5% increase seen at this concentration is used to normalize final results; therefore percentage reductions reported in the results to follow have all been adjusted for the effect of tetracycline on mtDNA-CN.

3.5 Dose-dependent induction of D1135A cell lines is unachievable at chosen ranges

The results from the first concentration range identify that treating cells with 0.5µg/mL of tetracycline results in a significant decrease in mtDNA-CN. However, mtDNA-CN appears to plateau when cells are treated with tetracycline doses higher than 0.5µg/mL. As such, the decision was made to tighten the concentration range around 0.5µg/mL tetracycline to see if there was a concentration-dependent response at lower tetracycline doses. To that end, D1135A cells were treated with 0.15, 0.30, 0.45, 0.60 and 0.75µg/mL of tetracycline for 24 hours, genomic DNA was extracted and mtDNA-CN estimation via qPCR was performed (Figure 15). Cells treated with: 0.15µg/mL had a 25% reduction in mtDNA-CN (p=2.84e-03); 0.30µg/mL had a 24% reduction in mtDNA-CN(p=1.32e-03); 0.45µg/mL had a 28% reduction in mtDNA-CN (p=3.21e-04); 0.60µg/mL had a 17% reduction in mtDNA-CN (p=0.011); and 0.75µg/mL had a 10% reduction in mtDNA-CN (p=0.068). Although the reduction of mtDNA-CN in cells treated with 0.75µg/mL is not significant, across all concentrations an overall 21% reduction of mtDNA-CN is seen (p=6.0e-03). This overall reduction in mtDNA-CN was not concentration dependent; mtDNA-CN of cells treated with 0.30, 0.45, 0.60 and 0.75 µg/mL tetracycline did not

differ from that of cells treated with 0.15µg/mL (p=0.979, p=0.517, p=0.321 and p=0.081, respectively).

Figure 15. qPCR estimation of mtDNA-CN in D1135A cells treated with 0.15, 0.30, 0.45, 0.60 and 0.75 µg/mL of tetracycline for 24 hours. All treatments resulted in significantly decreased mtDNA-CN (26%, p=8.54e-06). Percent reduction is adjusted for basal effect of tetracycline application on mtDNA-CN. Samples were run in technical triplicates. Asterisks indicate significance compared to D1135A POLG NC: * p<0.05, ** p<0.01, *** p<0.001, linear regression.

These results again suggest that treating cells with 0.15µg/mL of tetracycline resulted in a significant decrease in mtDNA-CN and that this decrease happens quickly and then plateaus even at low levels. The next range of doses was tightened around 0.15µg/mL to see if a stepwise dose response could be seen. To that end, D1135A cells were treated with 0.04, 0.08, 0.12, 0.16 and 0.20 µg/mL of tetracycline for 24 hours, and genomic DNA was extracted for mtDNA-CN estimation via qPCR (Figure 16). D1135A cell treated with: 0.04µg/mL tetracycline had a 37% reduction in mtDNA-CN (p=1.61e-05); 0.08µg/mL had a 42% reduction in mtDNA-CN (p=3.26e-06); 0.12µg/mL had a 50% reduction in mtDNA-CN (p=9.83e-07); 0.16µg/mL had a 45% reduction in mtDNA (p=1.40e-06); and 0.20µg/mL had a 39% reduction in mtDNA-CN (p=9.56e-06). Cells treated with 0.12µg/mL tetracycline had a significantly lower mtDNA-CN than cells treated with 0.04µg/mL (p=0.019), however mtDNA-CN of cells treated with 0.08µg/mL is not significantly lower than cells treated with 0.04µg/mL (p=0.293) or higher than cells treated with 0.12µg/mL (p=0.111). Although insignificant, there appears to be a small concentration-dependent effect on mtDNA-CN depletion seen in this range.
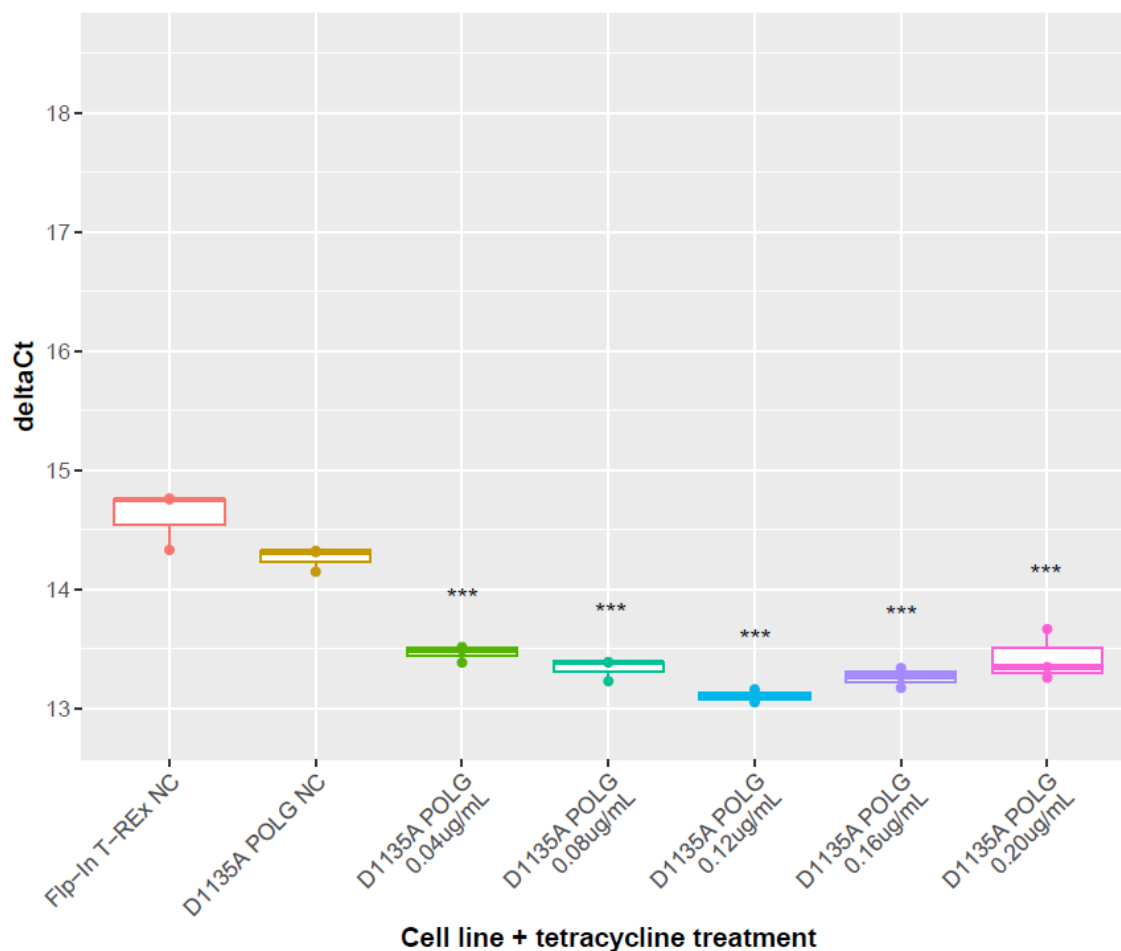
Figure 16. qPCR estimation of mtDNA-CN in D1135A cells treated with 0.04, 0.08, 0.12, 0.16 and 0.20 µg/mL of tetracycline for 24 hours. All doses resulted in a significant decrease of mtDNA-CN (47%, p=8.21e-08). Percent reduction is adjusted for basal effect of tetracycline application on mtDNA-CN. mtDNA-CN of cells treated with 0.12µg/mL of tetracycline was significantly lower than that of cells treated with 0.04µg/mL of tetracycline (p=0.019) but not cells treated with 0.08µg/mL (p=0.111). Samples were run in technical triplicates. Asterisks indicate significance compared to D1135A POLG NC: * p<0.05, ** p<0.01, *** p<0.001, linear regression.

A significant concentration-dependent reduction in mtDNA-CN was not seen for an individual range of concentrations. Looking across plates, treating cells with 0.5µg/mL of tetracycline reduced mtDNA-CN by 63%, 0.15µg/mL of tetracycline reduced mtDNA-CN by 25%, and 0.04µg/mL of tetracycline reduced mtDNA-CN by 37%. Thus, the final range of tetracycline concentration was determined to capture the lowest concentrations from each previous experiment. To that end, D1135A POLG cells were treated with 0.05, 0.15, 0.25, 0.35, 0.45 and 0.55 µg/mL of tetracycline for 24 hours and genomic DNA was extracted for mtDNA-CN estimation via qPCR analysis (Figure 17). D1135A cells treated with: 0.05µg/mL had a 46% reduction in mtDNA-CN (p=7.91e-13); 0.15µg/mL had a 38% reduction in mtDNA-CN (p=5.17e-10); 0.25µg/mL had a 41% reduction in mtDNA-CN (p=6.89e-10); 0.35µg/mL had a 38% reduction in mtDNA-CN (p=4.97e-10); 0.45µg/mL had a 39% reduction in mtDNA-CN (p=4.71e-09); and 0.55µg/mL had a 32% reduction in mtDNA-CN (p=5.26e-08).
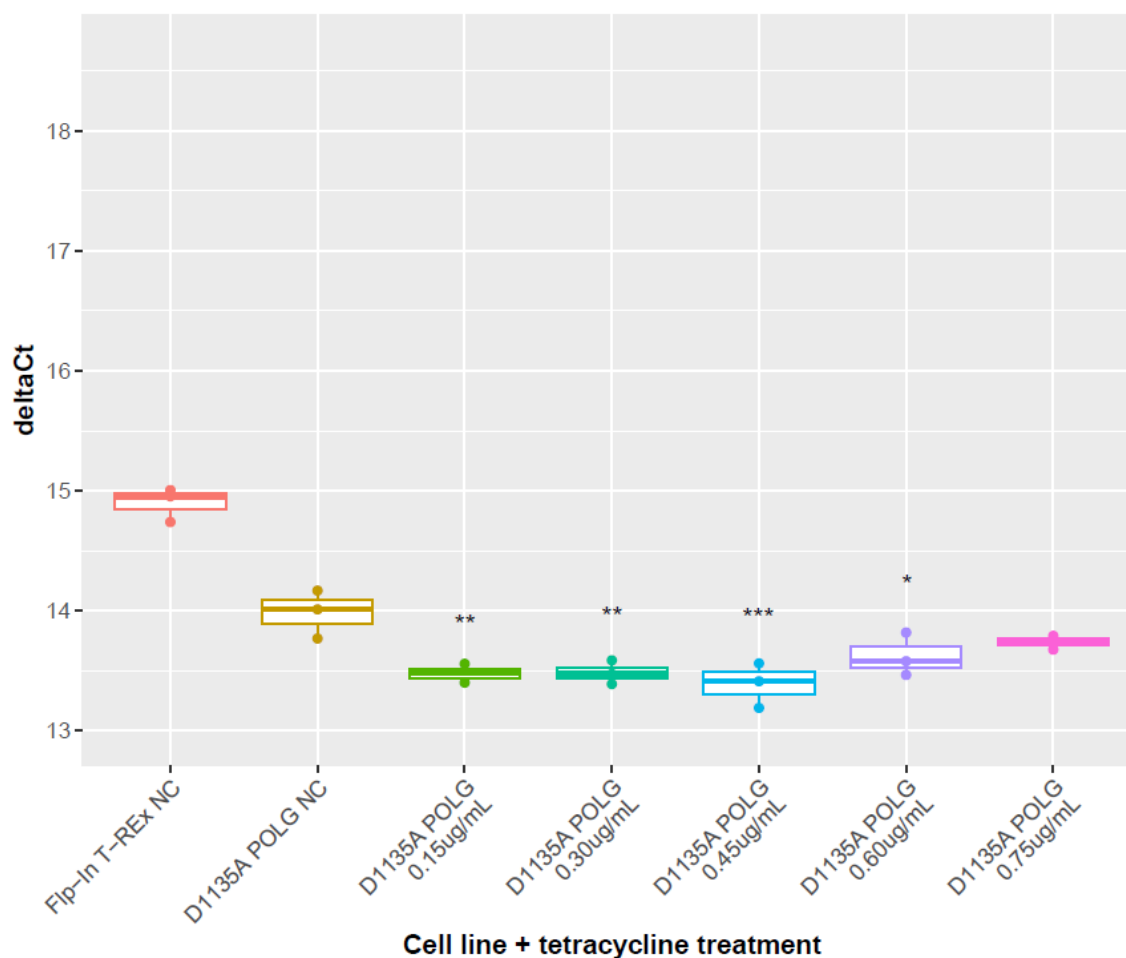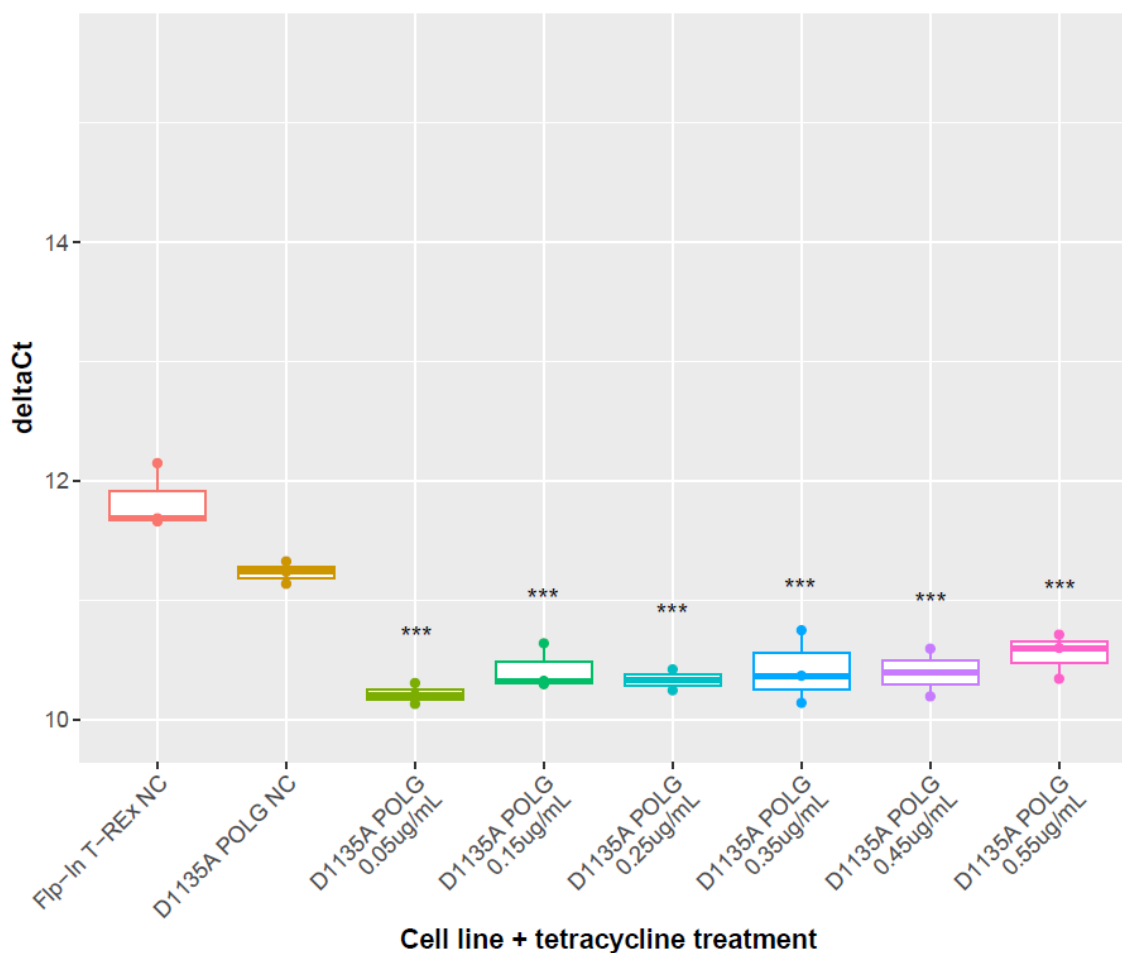
Figure 17. qPCR estimation of mtDNA-CN in D1135A POLG cells treated with 0.05, 0.15, 0.25, 0.35, 0.45 and 0.55 µg/mL of tetracycline for 24 hours. All doses resulted in a significant reduction of mtDNA-CN (p=2.2e-16). Percent reduction is adjusted for basal effect of tetracycline application on mtDNA-CN. Samples were run in biological and technical triplicates. Asterisks indicate significance compared to D1135A POLG NC: * p<0.05, ** p<0.01, *** p<0.001, linear regression.

Once again, a concentration-dependent response (p-value) could not be established despite our efforts. However, it was consistently demonstrated that mtDNA-CN is depleted following induction of D1135A with tetracycline.

3.6   D1135A POLG protein is expressed following tetracycline induction

Confirmation of integration of the gene of interest into the host cell genome does not necessarily guarantee protein expression of the gene of interest in the presence of tetracycline. To that end, D1135A POLG cells were treated with 0, 0.05, 0.15, 0.25, 0.35, 0.45, and 0.55 µg/mL of tetracycline for 24 hours. Flp-In^{TM} T-REx^{TM}-293 and untreated (NC) D1135A POLG cells were used as controls. Total protein lysates were extracted, quantified, diluted to equal concentrations, and denatured before being resolved on an 8% polyacrylamide gel and transferred to a 0.45um nitrocellulose membrane. Membranes were imaged after primary and secondary antibody incubations (Figure 18).

FLAG-tag band intensity was normalized to GAPDH band intensity and relative intensity of the bands were quantified as a measure of relative expression compared to D1135A POLG NC cells (no tet) (Figure 19). There is a significant increase in band intensity in all lanes containing protein from D1135A POLG cells treated with tetracycline (0.05µg/mL, p=0.0002; 0.15–0.35 µg/mL, p<0.001; 0.45µg/mL, p=0.0002; 0.55µg/mL, p=0.0001).

A concentration-dependent increase in band intensity was not seen. Band intensity in the 0.15µg/mL lane was significantly more intense than the 0.05µg/mL lane (p=9.44e-11, linear regression), but also significantly more intense than the 0.25µg/mL lane (p=4.10e-07). Further, the band intensity in the 0.45µg/mL lane is significantly less intense than both the 0.35µg/mL lane (p=5.11e-07) and the 0.55µg/mL lane (p=4.52e-10).
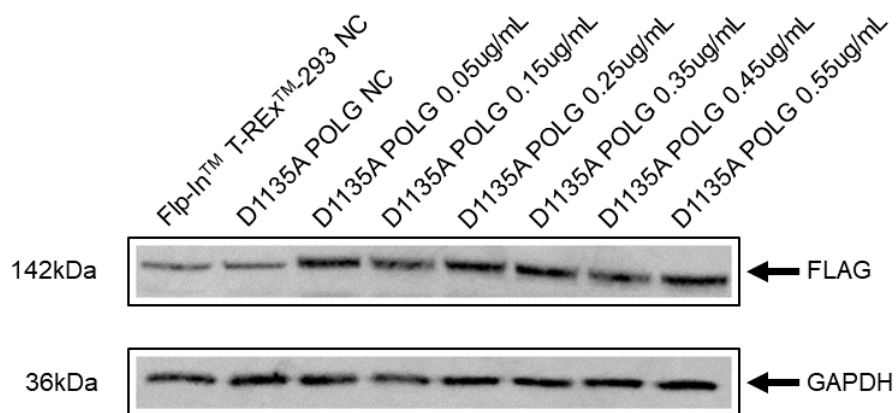
Figure 18. Treating D1135A POLG cells with tetracycline for 24 hours results in an increase in FLAG-tag abundance, suggesting an increase in D1135A POLG protein expression as D1135A POLG is tagged with 2x FLAG tags. Flp-In™ T-REx™-293 NC and D1135A POLG NC are controls.
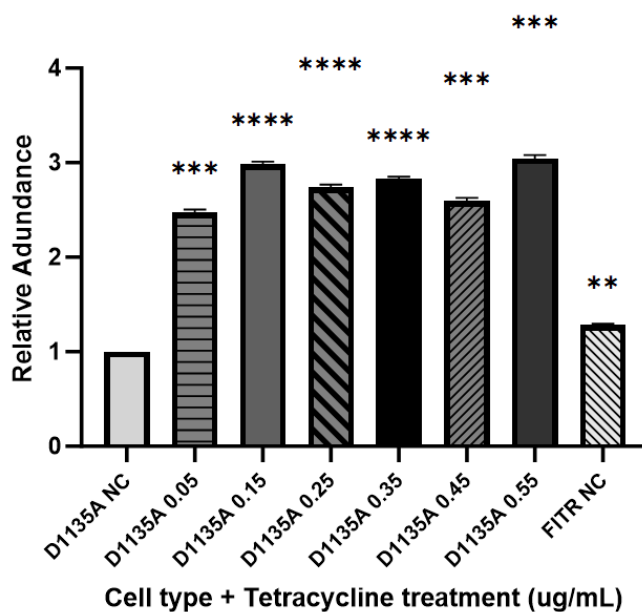
Figure 19. Relative abundance of FLAG protein bands, normalized to GAPDH protein bands, compared to D1135A NC cells. All tetracycline treatments resulted in a significant increase of D1135A POLG protein expression compared to D1135A NC cells. FITR: Flp-In™ T-REx™-293. Asterisks indicate significance: ** $p<0.01$, *** $p<0.001$, **** $p<0.0001$, one sample t-test.

Chapter 4

4   Discussion

Here, it is shown that a cell-line model whereby tetracycline-inducible expression of a polymerase-deficient dominant-negative DNA polymerase gamma (D1135A POLG) resulting in the depletion of mtDNA-CN has been successfully generated. Given the association between mtDNA-CN variation and the nuclear epigenome, this model has the potential for further exploration of mitochondrial-nuclear dynamics.

4.1   Confirming the presence of DN-POLG mutations in plasmid vectors

To use the Flp-In^{TM} T-Rex^{TM}-293 stable inducible expression system, the gene of interest must be cloned into the multiple cloning site of the pcDNA5/FRT/TO plasmid. Generation of the pcDNA5/FRT/TO expression plasmid containing the gene of interest can be achieved in-house or can be outsourced to other facilities. When generating the plasmid in-house, the gene of interest is produced via site-directed mutagenesis. It is essential for the gene of interest to be sequenced after site-directed mutagenesis to ensure no other mutations arose from the mutagenesis protocol. Therefore, to avoid potential sites of unexpected mutation others who have used the Flp-In^{TM} T-REx^{TM}-293 stable inducible expression system for D198A and D1135A POLG expression performed confirmatory sequencing (109,111,115). For this project, pcDNA5/FRT/TO expression plasmid generation was outsourced to Gene Art (Thermo Scientific) and the plasmids were confirmed via sequencing.

4.2   Confirming integration of pcDNA^{TM}5/FRT/TO vector in the Flp-In^{TM} T-REx^{TM}-293 genome

With the Flp-In^{TM} T-REx^{TM}-293 stable inducible expression system, cells exhibit hygromycin resistance upon successful integration of the gene of interest into the genome. Therefore, successfully integrated cells will grow in the presence of hygromycin in the growth media. Others who have used the Flp-In^{TM} T-REx^{TM}-293 expression system do not report confirming integration of their gene of interest at the genomic level, rather they report confirmation of integration via the growth of the cells in the presence of

hygromycin. However, it was of interest to amplify and sequence unique features of the post-integration genome to confirm integration of the exact mutations of interest into the Flp-In[TM] T-REx[TM]-293 host cell genome. While one can assume that the post-integration genome possesses its genomic features in the order stated, Here the features of the post-integration genome were successfully confirmed.

4.3   D1135A POLG induction leads to mtDNA-CN depletion

A previous study using the Flp-In[TM] T-REx[TM]-293 stable inducible expression system to express D1135A DN-POLG reported that 0.01µg/mL of tetracycline was sufficient to induce expression of the gene of interest and significantly deplete mtDNA-CN by ~70% (111). In addition, the manual for the expression system recommends treating cells with 1.0µg/mL of tetracycline to induce expression of your gene of interest (113). Other studies using the Flp-In[TM] T-REx[TM]-293 stable inducible expression system for the expression of a particular gene of interest reported using anywhere between 0.01–1.0µg/mL of tetracycline to induce expression (22,109,111). There was one study that reported using a variety of tetracycline concentrations to determine the concentration used for all experiments, but they did not see a dose-dependent effect (116). For these reasons I was curious if the expression of the gene of interest, and therefore mtDNA-CN depletion, would exert its effects in a concentration-dependent manner

For all concentration ranges, treating cells with the lowest concentration of tetracycline was sufficient to induce D1135A POLG expression (Figure 16) and significantly deplete mtDNA-CN (Figures 11, 13-15). Statistical analysis of the densitometry data from the Western blot reveals that increasing tetracycline concentration does not necessarily increase the quantity of D1135A POLG expression. One study reported treating Flp-In[TM] T-REx[TM]-293 cells with two tetracycline concentrations (1.0 or 10 µg/mL) for 24 hours and showed that protein expression of the gene of interest did not increase with tetracycline concentration (117). Other studies report treating Flp-In[TM] T-REx[TM]-293 cells with a single dose of tetracycline, either for a set time (116) or for a variety of time periods (118). To modulate the protein expression of the gene of interest, it may be required that cells are treated with tetracycline for less or more than 24 hours and for a variety of timeframes (i.e. 6 hour, 12 hour and 18 hour induction periods, as well as 48

hour, 72 hour, 96 hour induction periods), in addition to being treated with a variety of tetracycline concentrations. It is possible that doing so would have led to an even greater reduction in mtDNA-CN than was seen in the experiments presented here and thus a wider range within to generate a dose dependent response.

In these experiments, for the first concentration range (0.5–2.5 µg/mL tetracycline, figure 12) treating D1135A POLG cells with 0.5µg/mL resulted in a 63% reduction in mtDNA-CN. The reduction of mtDNA-CN induced by higher concentrations of tetracycline revealed that mtDNA-CN reduction is not concentration dependent: treating D1135A POLG cells with 1.0, 1.5, 2.0 or 2.5 µg/mL of tetracycline resulted in a 70%, 66%, 68% and 55% reduction in mtDNA-CN, respectively. The variation in mtDNA-CN depletion across this concentration range could potentially be explained by the dynamics between tetracycline-inducible mtDNA-CN depletion via D1135A POLG expression, and tetracycline exerting some small positive effects on mtDNA-CN, as seen in Figure 13.

Similar trends were seen in lower concentration ranges of tetracycline (0.15–0.75 µg/mL, 0.04–0.20 µg/mL, 0.05–0.55 µg/mL); when cells were treated with tetracycline, a decrease in mtDNA-CN is seen, but this decrease is not concentration-dependent. The variation in mtDNA-CN depletion seen in these concentration ranges is less likely to be explained by the dynamics of tetracycline. Flp-In™ T-REx™-293 cells treated with 0.5µg/mL of tetracycline had a 5% increase in mtDNA-CN (Figure 13). Although this increase in mtDNA-CN was significant, most concentrations within the lower concentration ranges do not reach 0.5µg/mL.

This variation in mtDNA-CN depletion could be explained by the dynamics of the cell cycle. During the S phase of the cell cycle mitochondrial fusion occurs, resulting in elongated mitochondria; during the G2 phase of the cell cycle, mitochondrial fission occurs, resulting in an abundance of fragmented mitochondria that will be divided equally among the two daughter cells after mitosis (119). This suggests that the dynamics of mtDNA-CN maintenance may coincide with the dynamics of mitochondrial structure during different phases of the cell cycle and thus future studies should explore the use of cell cycle synchronization during experimentation.

4.4   Results in experimental control cell lines suggest basal levels of induction

For all experiments where D1135A POLG cells were treated with tetracycline, native Flp-In™ T-REx™-293 cells were used as an additional control. In addition, D1135A POLG cells with no tetracycline were used as a control. As the host cell line, these cells have all the characteristics of D1135A POLG cells aside from stable inducible expression of DN-POLG. These cells were included as an additional control because it was anticipated that mtDNA-CN depletion in untreated D1135A POLG cells would be seen due to trace levels of tetracycline present in FBS and/or basal levels of expression in D1135A lines without induction. There are trace amounts of tetracycline in FBS due to standard agricultural practices, where livestock feed is supplemented with tetracycline to prevent common infections (120). Although the use of tet-free FBS was explored, samples of this FBS were just arriving in the lab around the time that I was finishing up my experimentation and thus this will be explored by a future student. Indeed, for each experiment, mtDNA-CN of untreated D1135A POLG cells was lower than the mtDNA-CN of Flp-In™ T-REx™-293 cells. This could be due to trace amounts of tetracycline in the media, as discussed. However, because the gene of interest is under control of a constitutive promoter, non-induced basal expression of D1135A POLG may also be the cause. The Western blot shows that untreated D1135A POLG cells are expressing the FLAG tag, but that does not distinguish whether there is induction of expression by trace tetracycline amounts, or non-induced basal levels of expression. Therefore, as stated, this question will be addressed with the use of tet-free FBS.

4.5   Tetracycline as an induction factor

Tetracyclines are a class of bacteriostatic antibiotics that function by inhibiting growth, specifically by binding to prokaryotic ribosomal subunit 30S, inhibiting protein synthesis (121). All tetracyclines have the same overall structure and function (122). The Flp-In™ T-REx™-293 manual states that both tetracycline and doxycycline are suitable to induce expression of the gene of interest (113). Doxycycline, another antibiotic of the tetracycline family, has been shown to inhibit mitochondrial protein synthesis in human fibroblasts treated with 10µg/mL of doxycycline for 5 days (123). Although this system

does not require such high concentrations to induce expression, evidence from four cell lines, including HEK293 cells, shows that treatment with 0.5 and 1.0 µg/mL of doxycycline impaired mitochondrial protein synthesis (124). Therefore, doxycycline should not be used for these experiments. Similarly, potential evidence of impaired mitochondrial protein synthesis in response to tetracycline treatment was seen here in Figure 14; where mtDNA-CN increased with increasing concentrations of tetracycline.

4.6   FLAG signal in native Flp-In™ T-REx™-293 cells

The presence of a protein band in Flp-In™ T-REx™-293 cells was identified when probed with the FLAG-tag antibody. Because these cells did not undergo a transfection protocol, this protein band was not expected to be seen. Given this finding, it was imperative to check and see if there were any genetic sequences arising from the integration of pFRT/lacZeo or pcDNA™6/TR plasmids in the generation of Flp-In™ T-REx™-293 cells that could bind the FLAG-tag antibody. Protein blast (NCBI) of all possible reading frames of the integrated plasmids against the FLAG tag (DYKDDDDK) did not reveal any areas of amino acid similarity with the human genome. However, the generation of the Flp-In™ T-REx™-293 cell lines could result in the *de novo* presence of a FLAG tag or similar in the proteome. In generating this cell line, the FRT site and TetR gene must be integrated into a random transcriptionally active region of the genome. The nature of recombination alters the host genome in the regions where the plasmids are integrated. It is possible that the DNA sequence of a transcriptionally active gene was altered to produce a protein product that contains an amino acid sequence that can bind with weak affinity to the FLAG tag antibody. To interrogate and confirm this possibility, PCR primers can be designed to anneal to and amplify the DNA sequence that corresponds with the FLAG epitope. Genomic DNA extracted from untreated Flp-In™ T-REx™-293 cells would then undergo a PCR protocol with the primers, and the PCR reaction would be run on an agarose gel to confirm presence of a DNA band. From there, DNA from the PCR reaction would be cleaned and prepared for Sanger sequencing, which would confirm the presence of a DNA sequence giving rise to a FLAG epitope that is detected using the FLAG tag antibody.

In the process of creating an inducible expression cell line using the Flp-In^{TM} T-REx^{TM}-293 system, the gene of interest must be amended with an epitope (tag) to detect the integrated and not the native protein product. Common epitopes include c-myc, His, and FLAG tags (125). Here, the gene of interest (DN-POLG) was amended with two FLAG tags at the C-terminus. The presence of the FLAG tag in D1135A POLG cells without tetracycline treatment was to be expected, due to trace amounts of tetracycline in standard FBS, and the potential for non-induced basal expression. One group in China reported low levels of expression of the gene of interest in the absence of doxycycline (126). Another group reported low expression levels of their gene of interest in the absence of doxycycline (127). Others who have used the FLAG tag in their Flp-In T-REx-293 system report no presence of the FLAG tag in cells that were not treated with tetracycline, however, this group does not specify which FBS has been used (128). It is thus possible that the lack of FLAG tag in untreated cells is due to tet-free FBS.

4.7   mtDNA-CN and the nuclear epigenome

There is an abundance of evidence linking mitochondrial DNA variation to the remodeling of the nuclear epigenomic landscape as discussed in section 1.3.1. Perhaps the most extensive studies of mtDNA variation on the nuclear epigenome have been in the context of mtDNA-CN. In our experimentation, treatment with tetracycline at any concentration was sufficient to significantly reduce mtDNA-CN; for cells treated with 0.5–2.5 µg/mL of tetracycline, a minimum mtDNA-CN decrease of 55% was seen in cells treated with 2.5µg/mL (Figure 12). For cells treated with 0.15–0.75µg/mL of tetracycline, a minimum mtDNA-CN decrease of 15% is seen in cells treated with 0.75µg/mL (Figure 13). For cells treated with 0.04–0.20 µg/mL of tetracycline, a minimum mtDNA-CN decrease of 42% is seen in cells treated with 0.04µg/mL (Figure 15).

Different levels of mtDNA-CN depletion results in differential levels of methylation of the nuclear epigenome. Enzymatic depletion of mtDNA-CN in mice zygotes resulted in a hypermethylation profile, specifically in the regulatory region of a transcriptional regulator of lipid metabolism, resulting in hepatic lipidosis later in life (129). An epigenome-wide association study across multiple cohorts and ethnicities revealed

differential methylation of specific nuclear CpGs is significantly associated with mtDNA-CN (25). The CpGs were subsequently confirmed in a *TFAM* knockout cell model of 18-fold mtDNA-CN reduction (25). Other models of mtDNA-CN depletion via inducible expression of D1135A POLG reveal hypermethylation in several differentially methylated regions (DMRs) and differentially expressed genes (DEGs) in response to various levels of mtDNA-CN depletion (60). In mice models where cardiac mtDNA-CN is depleted due to expression of a polymerase-deficient POLG, an overall hypermethylation profile is seen with 4,506 differentially methylated peaks (130).

Mitochondrial DNA copy number depletion is also associated with histone acetylation changes. Maintaining mtDNA-CN is required to maintain histone acetylation marks; D1135A POLG cells treated with doxycycline for 3, 6 or 9 days revealed the loss of histone acetylation marks which could be restored upon genetic restoration of the TCA cycle (22). Others reveal the same loss of histone acetylation marks at specific loci upon inducible expression of D1135A POLG, which could be restored by supplementing cells with TCA cycle intermediates (64).

Mitochondrial DNA copy number plays a significant role in the dynamics of the nuclear epigenome, however the mechanisms linking mtDNA-CN to the nuclear epigenome remains unclear. The hope is that the generated models in this thesis will be further optimized by future students to generate a number of step-wise changes in mtDNA-CN which will be used for downstream characterization of the nuclear epigenome at low, medium, and high levels of mtDNA-CN depletion.

4.8   Plans for characterization of DN-POLG cell lines in the future

As the metabolic hub of the cell, the activities of the mitochondrion have significant implications for the functioning of a cell. Aside from its crucial role in energy production, mitochondria have been shown to play a role in epigenetic processes, including DNA methylation and histone methylation and acetylation. Mitochondrial function maintains the flux of metabolites that are substrates and/or cofactors of epigenomic processes, including acetyl CoA, αKG, and NAD+.

The Castellani Lab is interested in the role mtDNA variation has in remodeling the nuclear epigenome, and how these factors contribute to the pathology of complex diseases. In the future, all DN-POLG cell lines (WT, D198A, D1135A) will be used to interrogate the effects of mtDNA variation on the nuclear epigenome in several facets. Heteroplasmy and mtDNA-CN variation are known to alter DNA methylation and histone acetylation (50). These cell lines can be utilized to discover precise epigenomic alterations resulting from mtDNA-CN and/or site-specific and global heteroplasmy. From there, RNA sequencing will be used to interrogate the effects of these epigenomic alterations, and global metabolomic profiles will be directly assayed to uncover mechanisms of action.

This is especially pertinent as what remains to be elucidated is the mechanism through which mtDNA variation alters the nuclear epigenome. While some mechanisms may be more apparent (i.e. decreasing mtDNA-CN leads to decreased TCA activity, reducing acetyl CoA levels and histone acetylation marks), overall it is unclear precisely how mtDNA variation alters the nuclear epigenome. It has been proposed that one possible mechanism is through the modulation of epigenome-modifying mitochondrial metabolites (23). However, mitochondrial function is implicated in several metabolic processes, and "mitochondrial" metabolites such as αKG and acetyl CoA can be generated elsewhere in the cell. As such, mitochondrial function may modulate other cellular processes and metabolites that are playing a significant role in the dynamics of the epigenomic landscape.

Others who use D198A and D1135A POLG to induce mtDNA variation in culture claim that altered POLG behaves in a dominant-negative fashion, however this is yet to be confirmed at the protein level. To confirm the dominant-negative designation attributed to these cell lines, co-immunoprecipitation (CoIP) can be performed. The catalytic subunit of POLG binds to two accessory POLG subunits to become a functional DNA polymerase. Using antibodies that target the wild-type and altered catalytic POLG subunit and antibodies that target the accessory subunits, CoIP will show if the wild-type or altered catalytic POLG subunit preferentially binds to the accessory subunits.

4.9 Limitations

Some limitations were identified over the course of this research project. One limitation in the DN-POLG cell lines is the overuse of antibiotics. The cell lines require two selection antibiotics and an induction antibiotic. The cell culture protocol used here also includes penicillin and streptomycin in the culture media. The overuse of antibiotics and other agents such as antifungals can alter gene expression and the chromatin landscape (131). Since these cell lines are to be used to interrogate the effects mtDNA variation has on the nuclear epigenome, which has implications for both gene expression and the chromatin landscape, antibiotic use and overuse should be minimized where possible. Another limitation of the DN-POLG cells is that they are polyclonal. A polyclonal cell population can exhibit several phenotypes that could have implications for mtDNA maintenance, mitochondrial function, and the nuclear epigenome. Single cell sorting of the polyclonal population was not performed here but could be performed in the future. Some other limitations were professional and personal obstacles arising from the global pandemic; isolation, illness, and supply shortages were some of the obstacles faced during the project.

4.10 Future Directions

Many factors contributing to the variation of mtDNA-CN depletion across qPCR plates (figures 12–16) will be addressed in the future. Tetracycline free FBS will be used to culture D1135A POLG cells before genomic DNA extraction for mtDNA-CN estimation, potentially eliminating the confounding variable of basal D1135A POLG expression without induction. D198A POLG cells will also be cultured in tetracycline free FBS. Further, evidence shows that expression of the D198A POLG exonuclease mutation does not alter mtDNA-CN (111) but what has yet to be analyzed is if expression of the D1135A POLG polymerase mutation alters mtDNA heteroplasmy. Whole genome sequencing of tetracycline treated D1135A POLG cells can be used to determine heteroplasmic load in this line. The results from such an experiment would be among the first to be reported in the literature.

The high variability in the reduction of mtDNA-CN in untreated D1135A POLG cells compared to Flp-In^{TM} T-REx^{TM}-293 cells, as well as the high variability in mtDNA-CN in treated compared to untreated D1135A POLG cells across all experiments could be the result of the nature of cell culture practices and cell culture dynamics. Tetracycline powder is stored in the dark at 4˚C to prevent degradation of the antibiotic. Similarly, cell culture media is stored in the dark at 4˚C. Cell culture media is warmed to 37˚C before its use with cells and is subject to multiple cycles of cold storage to warming. Tetracycline begins degrading at temperatures above 4˚C (132), so the multiple warming periods of cell culture media could degrade tetracycline such that it induces different levels of D1135A POLG expression and/or has varying effects on mtDNA-CN. In the future, this can be addressed by creating single-use aliquots of cell culture media, which will eliminate the constant cool/warm cycles and reduce incubation time, thus maintaining the integrity of the tetracycline molecule.

Further, as discussed above in section 4.3, the effect of varying timepoints of induction should be included in future experiments and may alter both the reproducibility and strength of the mtDNA-CN depletion.

The effects of the phases of the cell cycle on mtDNA-CN could be addressed by extracting genomic DNA from permeabilized cells sorted into populations based on the phase of the cell cycle. Although not particularly practical, this could uncover interesting information regarding the dynamics of the mitochondrial genome (rather than mitochondrial structure) during different phases of the cell cycle. Alternatively, cell-cycle synchronization could be performed during experimentation to reduce this potential confounding variable.

Chapter 5

5   Conclusion

An abundance of evidence has shown an association between mtDNA variation and the nuclear epigenome. While the mechanisms of this association have yet to be elucidated, there are many ways to study this association in *in vitro* models.

Here, stable inducible expression of polymerase deficient dominant-negative D1135A POLG was achieved via co-transfection of the pOG44 and pcDNA^{TM}5/FRT/TO vectors into the Flp-In^{TM} T-REx^{TM}-293 genome with post-integration selection. The D1135A cell line was used to assess the effects of tetracycline induction on D1135A expression, and mtDNA-CN. It was found that treating cells with tetracycline levels 0.15µg/mL or higher for 24 hours resulted in a significant and reproducible decrease in mtDNA-CN.

The stable inducible expression models created for this project will be used in the future by trainees of the Castellani Lab to interrogate the effects of mtDNA variation on the nuclear epigenome, transcriptome, and metabolome. Global 'omics data will aim to elucidate the biological mechanisms facilitating the association between mtDNA variation and nuclear epigenomic and transcriptomic changes.

References

1. Kastaniotis AJ, Autio KJ, Kerätär JM, Monteuuis G, Mäkelä AM, Nair RR, et al. Mitochondrial fatty acid synthesis, fatty acids and mitochondrial physiology. Biochim Biophys Acta Mol Cell Biol Lipids. 2017; 1862(1):39–48.

2. Hajnóczky G, Csordás G, Das S, Garcia-Perez C, Saotome M, Sinha Roy S, et al. Mitochondrial calcium signalling and cell death: approaches for assessing the role of mitochondrial Ca2+ uptake in apoptosis. Cell Calcium. 2006; 40(5–6):553–60.

3. Li X, Fang P, Mai J, Choi ET, Wang H, Yang X feng. Targeting mitochondrial reactive oxygen species as novel therapy for inflammatory diseases and cancers. J Hematol Oncol. 2013; 6:19.

4. Green DR. Apoptotic Pathways: The Roads to Ruin. Cell. 1998; 94(6):695–8.

5. Harris DA, Das AM. Control of mitochondrial ATP synthesis in the heart. Biochem. J. 1991; 280:561–573.

6. Golpich M, Amini E, Mohamed Z, Ali RA, Ibrahim NM, Ahmadiani A. Mitochondrial Dysfunction and Biogenesis in Neurodegenerative diseases: Pathogenesis and Treatment. CNS Neurosci Ther. 2017; 23:5–22.

7. Ahn CS, Metallo CM. Mitochondria as biosynthetic factories for cancer proliferation. Cancer Metab. 2015; 3(1):1–10.

8. Siasos G, Tsigkou V, Kosmopoulos M, Theodosiadis D, Simantiris S, Maria Tagkou N, et al. Mitochondria and cardiovascular diseases-from pathophysiology to treatment. Ann Transl Med. 2018; 6(12):256.

9. Ali AT, Boehme L, Carbajosa G, Seitan VC, Small KS, Hodgkinson A. Nuclear genetic regulation of the human mitochondrial transcriptome. Elife. 2019; 8:1–23.

10.   Horan MP, Gemmell NJ, Wolff JN. From evolutionary bystander to master manipulator: the emerging roles for the mitochondrial genome as a modulator of nuclear gene expression. Eur J Hum Gen. 2013; 21:1335–1337

11.   Zhang Y, Qu Y, Gao K, Yang Q, Shi B, Hou P, et al. High copy number of mitochondrial DNA (mtDNA) predicts good prognosis in glioma patients. Am J Cancer Res. 2015; 5(3):1207–1216.

12.   D'Erchia AM, Atlante A, Gadaleta G, Pavesi G, Chiara M, De Virgilio C, et al. Tissue-specific mtDNA abundance from exome data and its correlation with mitochondrial transcription, mass and respiratory activity. Mitochondrion. 2015; 20:13–21.

13.   Ashar FN, Moes A, Moore AZ, Grove ML, Chaves PHM, Coresh J, et al. Association of mitochondrial DNA levels with frailty and all-cause mortality. J Mol Med. 2015; 93(2):177–86.

14.   Takahashi PY, Jenkins GD, Welkie BP, McDonnell SK, Evans JM, Cerhan JR, et al. Association of mitochondrial DNA copy number with self-rated health status. Appl Clin Genet. 2018; 11:121–127.

15.   Herbst A, Lee CC, Vandiver AR, Aiken JM, McKenzie D, Hoang A, et al. Mitochondrial DNA deletion mutations increase exponentially with age in human skeletal muscle. Aging Clin Exp Res. 2021; 33(7):1811–1820.

16.   Nandakumar P, Tian C, O'Connell J, Hinds D, Paterson AD, Sondheimer N. Nuclear genome-wide associations with mitochondrial heteroplasmy. Sci Adv. 2021; 7:eabe7520.

17.   Payne BAI, Wilson IJ, Patrick YWM, Coxhead J, Deehan D, Horvath R, et al. Universal heteroplasmy of human mitochondrial DNA. Hum Mol Genet. 2013; 22(2):384–90.

18. Schaefer AM, McFarland R, Blakely EL, He L, Whittaker RG, Taylor RW, et al. Prevalence of mitochondrial DNA disease in adults. Ann Neurol. 2008; 63(1):35–9.

19. Stewart JB, Chinnery PF. The dynamics of mitochondrial DNA heteroplasmy: implications for human health and disease. Nat Rev Genet. 2015; 16:530–42.

20. Smiraglia D, Kulawiec M, Bistulfi G, Gupta S, Singh K. A novel role for mitochondria in regulating epigenetic modification in the nucleus. Cancer Biol Ther. 2008; 7(8):1182–1190.

21. Xiao M, Yang H, Xu W, Ma S, Lin H, Zhu H, et al. Inhibition of α-KG-dependent histone and DNA demethylases by fumarate and succinate that are accumulated in mutations of FH and SDH tumor suppressors. Genes Dev. 2012; 26(12):1326–38.

22. Martínez-Reyes I, Diebold LP, Kong H, Schieber M, Huang H, Hensley CT, et al. TCA Cycle and Mitochondrial Membrane Potential Are Necessary for Diverse Biological Functions. Mol Cell. 2016; 61(2):199–209.

23. Morin AL, Win PW, Lin AZ, Castellani CA. Mitochondrial genomic integrity and the nuclear epigenome in health and disease. Front Endocrinol (Lausanne). 2022;13:1–9.

24. Liu X, Zhang Y, Ni M, Cao H, Signer RAJ, Li D, et al. Regulation of mitochondrial biogenesis in erythropoiesis by mTORC1-mediated protein translation. Nat Cell Biol. 2017;19(6):626–38.

25. Castellani CA, Longchamps RJ, Sumpter JA, Newcomb CE, Lane JA, Grove ML, et al. Mitochondrial DNA copy number can influence mortality and cardiovascular disease via methylation of nuclear DNA CpGs. Genome Med. 2020; 12(1):84.

26. Wang P, Castellani CA, Yao J, Huan T, Bielak LF, Zhao W, et al. Epigenome-wide association study of mitochondrial genome copy number. Hum Mol Genet. 2022;31(2):309–19.

27. Janssen JJE, Grefte S, Keijer J, de Boer VCJ. Mito-Nuclear Communication by Mitochondrial Metabolites and Its Regulation by B-Vitamins. Front Physiol. 2019; 10:1–23.

28. Seo BJ, Yoon SH, Do JT. Mitochondrial dynamics in stem cells and differentiation. Int J Mol Sci. 2018;19(12).

29. Pfanner N, Warscheid B, Wiedemann N. Mitochondrial proteins: from biogenesis to functional networks. Nat Rev Mol Cell Biol. 2016; 20(5):267–284.

30. Sutendra G, Kinnaird A, Dromparis P, Paulin R, Stenson TH, Haromy A, et al. A Nuclear Pyruvate Dehydrogenase Complex Is Important for the Generation of Acetyl-CoA and Histone Acetylation. Cell. 2014; 158(1):84–97.

31. Laubichler MD, Davidson EH. Establishment of the Role of Nuclear Chromosomes in Development. Dev Biol. 2008; 314(1):1–11.

32. Nagaraj R, Sharpley MS, Chi F, Braas D, Zhou Y, Kim R, et al. Nuclear Localization of Mitochondrial TCA Cycle Enzymes as a Critical Step in Mammalian Zygotic Genome Activation. Cell. 2017; 168(1–2):210-223.e11.

33. Kazak L, Reyes A, Holt IJ. Minimizing the damage: Repair pathways keep mitochondrial DNA intact. Nat Rev Mol Cell Biol. 2012; 13:659–71.

34. Moretton A, Morel F, Macao B, Lachaume P, Ishak L, Lefebvre M, et al. Selective mitochondrial DNA degradation following double-strand breaks. PLoS One. 2017; 12(4):e0176795.

35. Pinto M, Pickrell AM, Wang X, Bacman SR, Yu A, Hida A, et al. Transient mitochondrial DNA double strand breaks in mice cause accelerated aging phenotypes in a ROS-dependent but p53/p21-independent manner. Cell Death Differ. 2017; 24(2):288–99.

36. Tigano M, Vargas DC, Tremblay-Belzile S, Fu Y, Sfeir A. Nuclear sensing of breaks in mitochondrial DNA enhances immune surveillance. Nature. 2021;591(7850):477–81.

37. Zhu D, Wu X, Zhou J, Li X, Huang X, Li J, et al. NuRD mediates mitochondrial stress–induced longevity via chromatin remodeling in response to acetyl-CoA level. Sci Adv. 2020;6(31):1–12.

38. Tian Q, Moore AZ, Oppong R, Ding J, Zampino M, Fishbein KW, et al. Mitochondrial DNA copy number and heteroplasmy load correlate with skeletal muscle oxidative capacity by P31 MR spectroscopy. Aging Cell. 2021;20(11):1–6.

39. Kauppila JHK, Baines HL, Bratic A, Simard ML, Freyer C, Mourier A, et al. A Phenotype-Driven Approach to Generate Mouse Models with Pathogenic mtDNA Mutations Causing Mitochondrial Disease. Cell Rep. 2016;16(11):2980–90.

40. Larsen S, Nielsen J, Hansen CN, Nielsen LB, Wibrand F, Stride N, et al. Biomarkers of mitochondrial content in skeletal muscle of healthy young human subjects. J Physiol. 2012;590(14):3349–60.

41. Radzak SMA, Khair SZNM, Ahmad F, Patar A, Idris Z, Yusoff AAM. Insights regarding mitochondrial DNA copy number alterations in human cancer. Int J Mol Med. 2022; 50(2):104.

42. Tian M, Bao H, Martin FL, Zhang J, Liu L, Huang Q, et al. Association of DNA methylation and mitochondrial DNA copy number with human semen quality. Biol Reprod. 2014;91(4):1–8.

43. Bao XR, Ong SE, Goldberger O, Peng J, Sharma R, Thompson DA, et al. Mitochondrial dysfunction remodels one-carbon metabolism in human cells. Elife. 2016;5:1–24.

44. Chen Q, Kirk K, Shurubor YI, Zhao D, Arreguin AJ, Shahi I, et al. Rewiring of Glutamine Metabolism Is a Bioenergetic Adaptation of Human Cells with Mitochondrial DNA Mutations. Cell Metab. 2018;27(5):1007-1025.e5.

45. Lozoya OA, Xu F, Grenet D, Wang T, Grimm SA, Godfrey V, et al. Single Nucleotide Resolution Analysis Reveals Pervasive, Long-Lasting DNA Methylation Changes by Developmental Exposure to a Mitochondrial Toxicant. Cell Rep. 2020;32(11):108131.

46. Moore LD, Le T, Fan G. DNA Methylation and Its Basic Function. Neuropsychopharmacology. 2013; 38(1):23–38.

47. Irvine RA, Lin IG, Hsieh CL. DNA Methylation Has a Local Effect on Transcription and Histone Acetylation. Mol Cell Biol. 2002;22(19):6689–96.

48. Miller JL, Grant PA, Miller JL, Grant PA. The Role of DNA Methylation and Histone Modifications in Transcriptional Regulation in Humans. Subcell Biochem. 2013;61:289–317.

49. Rakyan VK, Down TA, Balding DJ. Epigenome-wide association studies for common human diseases. Nat Rev Genet. 2011;12:529.

50. Matilainen O, Quirós PM, Auwerx J. Mitochondria and Epigenetics – Crosstalk in Homeostasis and Stress. 2017;27(6):453–63.

51. Oluwayiose OA, Josyula S, Houle E, Marcho C, Whitcomb B, Rahil T, et al. Association between sperm mitochondarial DNA copy number and nuclear DNA methylation. Epigenomics. 2020;12(24):2141–53.

52. Dhar SK, Scott T, Wang C, Fan TWM, St Clair DK. Mitochondrial superoxide targets energy metabolism to modulate epigenetic regulation of NRF2-mediated transcription. Free Radic Biol Med. 2022;179:181–9.

53. Liu X, Zhang Y, Ni M, Cao H, Signer RAJ, Li D, et al. Regulation of mitochondrial biogenesis in erythropoiesis by mTORC1-mediated protein translation. Nat Cell Biol. 2017;19(6):626–38.

54. Solomon WL, Hector SBE, Raghubeer S, Erasmus RT, Kengne AP, Matsha TE. Genome-wide DNA methylation and lncrna-associated DNA methylation in metformin-treated and-untreated diabetes. Epigenomes. 2020;4(3):19.

55. Cuyàs E, Fernández-Arroyo S, Verdura S, García RÁF, Stursa J, Werner L, et al. Metformin regulates global DNA methylation via mitochondrial one-carbon metabolism. Oncogene. 2018;37(7):963–70.

56. Ducker GS, Rabinowitz JD. One-Carbon Metabolism in Health and Disease. Cell Metab. 2017;25(1):27–42.

57. F. C. Lopes A. Mitochondrial metabolism and DNA methylation: a review of the interaction between two genomes. Clin Epigenetics. 2020;12(1):1–13.

58. Ducker GS, Rabinowitz JD. One-Carbon Metabolism in Health and Disease. Cell Metab. 2017;25(1):27–42.

59. Bao XR, Ong SE, Goldberger O, Peng J, Sharma R, Thompson DA, et al. Mitochondrial dysfunction remodels one-carbon metabolism in human cells. Elife. 2016;5:1–24.

60. Lozoya OA, Martinez-Reyes I, Wang T, Grenet D, Bushel P, Li J, et al. Mitochondrial nicotinamide adenine dinucleotide reduced (NADH) oxidation links the tricarboxylic acid (TCA) cycle with methionine metabolism and nuclear DNA methylation. PLoS Biol. 2018;16(4):e2005707.

61. Kottakis F et al. LKB1 loss links serine metabolism to DNA methylation and tumourigenesis. Nature. 2016;539(7629):390–5.

62. Lozoya OA, Martinez-Reyes I, Wang T, Grenet D, Bushel P, Li J, et al. Mitochondrial nicotinamide adenine dinucleotide reduced (NADH) oxidation links the tricarboxylic acid (TCA) cycle with methionine metabolism and nuclear DNA methylation. PLoS Biol. 2018;16(4):e2005707.

63.   Cluntun AA, Huang H, Dai L, Liu X, Zhao Y, Locasale JW. The rate of glycolysis quantitatively mediates specific histone acetylation sites. Cancer Metab. 2015;3(1):1–12.

64.   Lozoya OA, Wang T, Grenet D, Wolfgang TC, Sobhany M, Da Silva DG, et al. Mitochondrial acetyl-CoA reversibly regulates locusspecific histone acetylation and gene expression. Life Sci Alliance. 2019;2(1):1–15.

65.   Prokesch A, Pelzmann HJ, Pessentheiner AR, Huber K, Madreiter-Sokolowski CT, Drougard A, et al. N-acetylaspartate catabolism determines cytosolic acetyl-CoA levels and histone acetylation in brown adipocytes. Sci Rep. 2016;6:1–12.

66.   Zhao S, Torres AM, Henry RA, Trefely S, Wallace M, Lee J V., et al. ATP-Citrate Lyase Controls a Glucose-to-Acetate Metabolic Switch. Cell Rep. 2016;17(4):1037–52.

67.   Sun X, St John JC. Modulation of mitochondrial DNA copy number in a model of glioblastoma induces changes to DNA methylation and gene expression of the nuclear genome in tumours. Epigenetics Chromatin. 2018;11(1):1–18.

68.   Figueroa ME, Abdel-Wahab O, Lu C, Ward PS, Patel J, Shih A, et al. Leukemic IDH1 and IDH2 Mutations Result in a Hypermethylation Phenotype, Disrupt TET2 Function, and Impair Hematopoietic Differentiation. Cancer Cell. 2010;18(6):553–67.

69.   Qiu Z, Lin AP, Jiang S, Elkashef SM, Myers J, Srikantan S, et al. MYC Regulation of D2HGDH and L2HGDH Influences the Epigenome and Epitranscriptome. Cell Chem Biol. 2020;27(5):538-550.e7.

70.   Dhar SK, Scott T, Wang C, Fan TWM, St Clair DK. Mitochondrial superoxide targets energy metabolism to modulate epigenetic regulation of NRF2-mediated transcription. Free Radic Biol Med. 2022;179:181–9.

71. Spyrou J, Gardner DK, Harvey AJ. Metabolomic and Transcriptional Analyses Reveal Atmospheric Oxygen During Human Induced Pluripotent Stem Cell Generation Impairs Metabolic Reprogramming. Stem Cells. 2019;37(8):1042–56.

72. Amsalem Z, Arif T, Shteinfer-Kuzmine A, Chalifa-Caspi V, Shoshan-Barmatz V. The mitochondrial protein vdac1 at the crossroads of cancer cell metabolism: The epigenetic link. Cancers (Basel). 2020;12(4).

73. Alcolado JC, Majid A, Brockington M, Sweeney MG, Morgan R, Rees A, et al. Mitochondrial gene defects in patients with NIDDM. Diabetologia. 1994;(37):372–6.

74. Mimaki M, Ikota A, Sato A, Komaki H, Akanuma J, Nonaka I, et al. A double mutation (G11778A and G12192A) in mitochondrial DNA associated with Leber's hereditary optic neuropathy and cardiomyopathy. J Hum Genet. 2003;48(1):47–50.

75. Côté HCF, Brumme ZL, Craib KJP, Alexander CS, Wynhoven B, Ting L, et al. Changes in Mitochondrial DNA as a Marker of Nucleoside Toxicity in HIV-Infected Patients. New England Journal of Medicine. 2002;346(11):811–20.

76. Souren NYP, Gerdes LA, Kümpfel T, Lutsik P, Klopstock T, Hohlfeld R, et al. Mitochondrial DNA Variation and Heteroplasmy in Monozygotic Twins Clinically Discordant for Multiple Sclerosis. Hum Mutat. 2016;37(8):765–75.

77. Stathopoulos S, Gaujoux R, Lindeque Z, Mahony C, Van Der Colff R, Van Der Westhuizen F, et al. DNA Methylation Associated with Mitochondrial Dysfunction in a South African Autism Spectrum Disorder Cohort. Autism Research. 2020;13(7):1079–93.

78. Li H, Bi R, Fan Y, Wu Y, Tang Y, Li Z, et al. mtDNA Heteroplasmy in Monozygotic Twins Discordant for Schizophrenia. Mol Neurobiol. 2017;54(6):4343–52.

79. Kujoth GC, Hiona A, Pugh TD, Someya S, Panzer K, Wohlgemuth SE, et al. Mitochondrial DNA Mutations, Oxidative Stress, and Apoptosis in Mammalian Aging. Science. 2005;309(5733):481–4.

80. Thakur N, Sharma AK, Singh H, Singh S. Role of Mitochondrial DNA (mtDNA) Variations in Cancer Development: A Systematic Review. Cancer Invest. 2020;38(7):375–93.

81. Potter M, Newport E, Morten KJ. The Warburg effect: 80 years on. Biochem Soc Trans. 2016; 44(5):1499–1505.

82. Bordoni L, Petracci I, Mlodzik-Czyzewska M, Malinowska AM, Szwengiel A, Sadowski M, et al. Mitochondrial DNA and Epigenetics: Investigating Interactions with the One-Carbon Metabolism in Obesity. Oxid Med Cell Longev. 2022;2022.

83. Zheng LD, Linarelli LE, Liu L, Wall SS, Greenawald MH, Seidel RW, et al. Insulin resistance is associated with epigenetic and genetic regulation of mitochondrial DNA in obese humans. Clin Epigenetics. 2015;7(1):1–9.

84. Liu X, Longchamps RJ, Wiggins KL, Raffield LM, Bielak LF, Zhao W, et al. Association of mitochondrial DNA copy number with cardiometabolic diseases. Cell Genomics. 2021;1(1):100006.

85. Hong YS, Longchamps RJ, Zhao D, Castellani CA, Loehr LR, Chang PP, et al. Mitochondrial DNA Copy Number and Incident Heart Failure. Circulation. 2020;141(22):1823–5.

86. Zhao D, Bartz TM, Sotoodehnia N, Post WS, Heckbert SR, Alonso A, et al. Mitochondrial DNA copy number and incident atrial fibrillation. BMC Med. 2020;18(1):246.

87. Haas J, Frese KS, Sedaghat-Hamedani F, Kayvanpour E, Tappu R, Nietsch R, et al. Energy metabolites as biomarkers in ischemic and dilated cardiomyopathy. Int J Mol Sci. 2021;22(4):1–13.

88. Ikeda M, Ide T, Fujino T, Arai S, Saku K, Kakino T, et al. Overexpression of TFAM or twinkle increases mtDNA copy number and facilitates cardioprotection associated with limited mitochondrial oxidative stress. PLoS One. 2015;10(3):1–19.

89. Lewis W, Day BJ, Kohler JJ, Hosseini SH, Chan SSL, Green EC, et al. Decreased mtDNA, oxidative stress, cardiomyopathy, and death from transgenic cardiac targeted human mutant polymerase γ. Laboratory Investigation. 2007;87(4):326–35.

90. Koczor CA, Ludlow I, Fields E, Jiao Z, Ludaway T, Russ R, et al. Mitochondrial polymerase gamma dysfunction and aging cause cardiac nuclear DNA methylation changes. Physiol Genomics. 2016;48(4):274–80.

91. Zhang Y, Liu X, Wiggins KL, Kurniansyah N, Guo X, Rodrigue AL, et al. Association of Mitochondrial DNA Copy Number With Brain MRI Markers and Cognitive Function: A Meta-analysis of Community-Based Cohorts. Neurology. 2023;100(18):e1930–43.

92. Jędrak P, Krygier M, Tońska K, Drozd M, Kaliszewska M, Bartnik E, et al. Mitochondrial DNA levels in Huntington disease leukocytes and dermal fibroblasts. Metabolic Brain Disorders. 2017;32:1237–47.

93. Pyle A, Anugrha H, Kurzawa-Akanbi M, Yarnall A, Burn D, Hudson G. Reduced mitochondrial DNA copy number is a biomarker of Parkinson's disease. Neurobiol Aging. 2015;38:216.e7-216.e10.

94. Fries GR, Bauer IE, Scaini G, Wu MJ, Kazimi IF, Valvassori SS, et al. Accelerated epigenetic aging and mitochondrial DNA copy number in bipolar disorder. Transl Psychiatry. 2017;7(12).

95. Fries GR, Bauer IE, Scaini G, Valvassori SS, Walss-Bass C, Soares JC, et al. Accelerated hippocampal biological aging in bipolar disorder. Bipolar Disord. 2020;22(5):498–507.

96. Chung JK, Lee SY, Park M, Joo EJ, Kim SA. Investigation of mitochondrial DNA copy number in patients with major depressive disorder. Psychiatry Res. 2019;282.

97. Win PW, Singh SM, Castellani CA. Mitochondrial DNA Copy Number and Heteroplasmy in Monozygotic Twins Discordant for Schizophrenia. Twin Research and Human Genetics. 2023;26:280–9.

98. von Wurmb-Schwark N, Ringleb A, Schwark T, Broese T, Weirich S, Schlaefke D, et al. The effect of chronic alcohol consumption on mitochondrial DNA mutagenesis in human blood. Mutation Research/Fundamental and Molecular Mechanisms of Mutagenesis. 2008;637(1–2):73–9.

99. Pirini F, Guida E, Lawson F, Mancinelli A, Guerrero-Preston R. Nuclear and mitochondrial DNA alterations in newborns with prenatal exposure to cigarette smoke. Int J Environ Res Public Health. 2015;12(2):1135–55.

100. Peng G, Xi Y, Bellini C, Pham K, Zhuang ZW, Yan Q, et al. Nicotine dose-dependent epigenomic-wide DNA methylation changes in the mice with long-term electronic cigarette exposure. Am J Cancer Res. 2022; 12(8):3679–3692.

101. Kupsco A, Sanchez-Guerra M, Amarasiriwardena C, Brennan KJM, Estrada-Gutierrez G, Svensson K, et al. Prenatal manganese and cord blood mitochondrial DNA copy number: Effect modification by maternal anemic status. Environ Int. 2019;126:484–93.

102. Cao X, Li J, Cheng L, Deng Y, Li Y, Yan Z, et al. The associations between prenatal exposure to polycyclic aromatic hydrocarbon metabolites, umbilical cord blood mitochondrial DNA copy number, and children's neurobehavioral development. Environmental Pollution. 2020;265:114594.

103. Petit C, Mathez D, Barthelemy C, Leste-Lasserre T, Naviaux RK, Sonigo P, et al. Quantitation of Blood Lymphocyte Mitochondrial DNA for the Monitoring of Antiretroviral Drug-Induced Mitochondrial DNA Depletion. JAIDS Journal of Acquired Immune Deficiency Syndromes. 2003;33(4):461–9.

104. Mendoza-Ortega JA, Reyes-Muñoz E, Nava-Salazar S, Rodríguez-Martínez S, Parra-Hernández SB, Schnaas L, et al. Mitochondrial dna copy number adaptation as a biological response derived from an earthquake at intrauterine stage. Int J Environ Res Public Health. 2021;18(22):1–10.

105. Exton JH. Regulation of gluconeogenesis by glucocorticoids. Monogr Endocrinol. 1979;12:535–46.

106. Alhassen S, Chen S, Alhassen L, Phan A, Khoudari M, De Silva A, et al. Intergenerational trauma transmission is associated with brain metabotranscriptome remodeling and mitochondrial dysfunction. Commun Biol. 2021;4(1).

107. Liu B, Song L, Zhang L, Wu M, Wang L, Cao Z, et al. Prenatal aluminum exposure is associated with increased newborn mitochondrial DNA copy number. Environmental Pollution. 2019;252:330–5.

108. Graziewicz MA, Longley MJ, Copeland WC. DNA polymerase γ in mitochondrial DNA replication and repair. Chemical Reviews. 2006; 106:383–405.

109. Jazayeri M, Andreyev A, Will Y, Ward M, Anderson CM, Clevenger W. Inducible expression of a dominant negative DNA polymerase-γ depletes mitochondrial DNA and produces a ρ0 phenotype. Journal of Biological Chemistry. 2003;278(11):9823–30.

110. Martínez-Reyes I, Chandel NS. Mitochondrial TCA cycle metabolites control physiology and disease. Nat Commun. 2020;11(1):1–11.

111. Wanrooij S, Goffart S, Pohjoismäki JLO, Yasukawa T, Spelbrink JN. Expression of catalytic mutants of the mtDNA helicase Twinkle and polymerase POLG causes distinct replication stalling phenotypes. Nucleic Acids Res. 2007;35(10):3238–51.

112. Saneto RP, Cohen BH, Copeland WC, Naviaux RK. Alpers-huttenlocher syndrome. Pediatric Neurology. 2013;48:167–78.

113. Life Technologies Corporation. Flp-In^TM T-REx^TM Core Kit For Generating Stable, Inducible Mammalian Expression Cell Lines by Flp Recombinase-Mediated Integration. User guide [Internet]. 2012;(25):1–9. Available from: http://tools.lifetechnologies.com/content/sfs/manuals/flpintrex_man.pdf

114. Hsieh AYY, Budd M, Deng D, Gadawska I, Côté HCF. A Monochrome Multiplex Real-Time Quantitative PCR Assay for the Measurement of Mitochondrial DNA Content. Journal of Molecular Diagnostics. 2018;20(5):612–20.

115. Spelbrink JN, Toivonen JM, Hakkaart GAJ, Kurkela JM, Cooper HM, Lehtinen SK, et al. In vivo functional analysis of the human mitochondrial DNA polymerase POLG expressed in cultured human cells. Journal of Biological Chemistry. 2000;275(32):24818–28.

116. Venneri M, Vezzi V, Mise A Di, Ranieri M, Centrone M, Tamma G, et al. Novel signalling pathways in nephrogenic syndrome of inappropriate antidiuresis: functional implication of site-specific AQP2 phosphorylation Key points. J Physiol. 2023;1–21.

117. Kudo TA, Kanetaka H, Watanabe A, Okumoto A, Asano M, Zhang Y, et al. Investigating bone morphogenetic protein (BMP) signaling in a newly established human cell line expressing BMP receptor type II. Tohoku Journal of Experimental Medicine. 2010;222(2):121–9.

118. Canals M, Milligan G. Constitutive activity of the cannabinoid CB1 receptor regulates the function of co-expressed Mu opioid receptors. Journal of Biological Chemistry. 2008;283(17):11424–34.

119. Mishra P, Chan DC. Mitochondrial dynamics and inheritance during cell division, development and disease. Nature Publishing Group. 2014;15.

120. Gustafson RH. Use of Antibiotics in Livestock and Human Health Concerns. J Dairy Sci. 1991;74(4):1428–32.

121. Chopra I, Roberts M. Tetracycline Antibiotics: Mode of Action, Applications, Molecular Biology, and Epidemiology of Bacterial Resistance. Microbiology and Molecular Biology Reviews. 2001;65(2):232–60.

122. Hlavka JJ, Boothe JH. The tetracyclines. Prog Drug Res. 1973;17:210–40.

123. Dijk SN, Protasoni M, Elpidorou M, Kroon AM, Taanman JW. Mitochondria as target to inhibit proliferation and induce apoptosis of cancer cells: the effects of doxycycline and gemcitabine. Sci Rep. 2020 Dec 1;10(1).

124. Moullan N, Mouchiroud L, Wang X, Ryu D, Williams EG, Mottis A, et al. Tetracyclines disturb mitochondrial function across eukaryotic models: A call for caution in biomedical research. Cell Rep. 2015;10(10):1681–91.

125. Fritze CE, Anderson TR. Epitope tagging: General method for tracking recombinant proteins BT - Applications of Chimeric Genes and Hybrid Proteins - Part B: Cell Biology and Physiology. Applications of Chimeric Genes and Hybrid Proteins - Part B: Cell Biology and Physiology. 2000 ; 327(1987):3–16.

126. Chen LQ, Wang YN, Li DY, Xu LY, Li LJ, Li ZH, et al. Construction of a Stable Expression Cell Line of Human Phospholamban. J Forensic Med. 2021 Oct 25;37(5):615–20.

127. Saran C, Ho H, Honkakoski P, Brouwer KLR. Effect of mTOR inhibitors on sodium taurocholate cotransporting polypeptide (NTCP) function in vitro. Front Pharmacol. 2023;14.

128. Béganton B, Coyaud E, Laurent EMN, Mangé A, Jacquemetton J, Le Romancer M, et al. Proximal Protein Interaction Landscape of RAS Paralogs. Cancers (Basel). 2020 Nov 11;12(11):3326.

129. Wang Y, Wang X, Long Q, Liu Y, Yin T, Sirota I, et al. Reducing embryonic mtDNA copy number alters epigenetic profile of key hepatic lipolytic genes and causes abnormal lipid accumulation in adult mice. FEBS Journal. 2021;288(23):6828–43.

130. Koczor CA, Ludlow I, Fields E, Jiao Z, Ludaway T, Russ R, et al. Mitochondrial polymerase gamma dysfunction and aging cause cardiac nuclear DNA methylation changes. Physiol Genomics. 2016;48(4):274–80.

131. Ryu AH, Eckalbar WL, Kreimer A, Yosef N, Ahituv N. Use antibiotics in cell culture with caution: genome-wide identification of antibiotic-induced changes in gene expression and regulation. Sci Rep. 2017;7:7533.

132. Yu Y, Chen L, fang Y, Jia X, Chen J. High temperatures can effectively degrade residual tetracyclines in chicken manure through composting. J Hazard Mater. 2019; 380.

Curriculum Vitae

Name: Amanda Louise Morin

Post-secondary
Education and
Degrees:
         University of Western Ontario
London, Ontario, Canada
2013-2019 BHSc

         The University of Western Ontario
London, Ontario, Canada
2019-2021 BSc

Honours and
Awards:
         Western Graduate Research Scholarship
2021-2023

         Ontario Graduate Scholarship
2022-2023

Related Work
Experience
         Graduate Teaching Assistant
The University of Western Ontario
2021-2022

Publications:
Morin AL, Win PW, Lin AZ, Castellani CA. Mitochondrial genomic integrity and the nuclear epigenome in health and disease. *Front Endocrinol* (2022) 13:1059085. doi: 10.3389/fendo.2022.1059085

Win PW, Nyugen J, Morin AL, Newcomb CE, Singh SM, Gomaa N, Castellani CA. Simultaneous assessment of mitochondrial DNA copy number and nuclear epigenetic age towards predictive models of development and aging. *BMC Research Notes* (Accepted)

Presentations:
Promoting Reconciliation among Graduate Students via Advocacy, Collaboration, and Education (2023) 8th Annual Building Reconciliation Forum

Epigenomic And Transcriptomic Profiles in Inducible Models of Mitochondrial DNA Copy Number Depletion and Heteroplasmic Burden (2022) 13th International Conference of Environmental Mutagens (ICEM) and the 53rd Annual Meeting of the Environmental Mutagenesis and Genomics Society (EMGS)

Posters:
The effect of *in vitro* models of mitochondrial DNA variation on the nuclear epigenome and transcriptome (2023) Pathology and Laboratory Medicine Research Day.

<u>Epigenomic and Transcriptomic Profiles in Inducible Models of Mitochondrial DNA Copy Number and Heteroplasmic Burden</u> (2022) Pathology and Laboratory Medicine's Research Day.

Awards:

2022–2023 — Ontario Graduate Scholarship

2022 — Head and Heart Research Fellowship

2021–2023 — Western Graduate Research Scholarship

2021 — Head and Heart Research Fellowship

2020 — EMGS Undergraduate Research Award

2020 — Head and Heart Research Fellowship